RESEARCH PAPER

PCCP
www.rsc.org/pccp

Effect of the self-interaction error for three-electron bonds: On the development of new exchange-correlation functionals

Jürgen Gräfenstein, Elfi Kraka and Dieter Cremer*

Theoretical Chemistry, Göteborg University, Box 460, SE-405 30, Göteborg, Sweden

Received 24th September 2003, Accepted 12th January 2004
First published as an Advance Article on the web 26th February 2004

The dissociation behavior as well as the equilibrium properties of radical cations with three-electron bonds, namely $He_2^{+\bullet}$, $N_2H_6^{+\bullet}$, $O_2H_4^{+\bullet}$, $F_2H_2^{+\bullet}$, and $Ne_2^{+\bullet}$ are investigated using standard and self-interaction-corrected density functional theory (SIC-DFT) in connection with a variety of pure and hybrid exchange-correlation (XC) functionals. The impact of the self-interaction error (SIE) on the results of standard DFT is analyzed considering the individual orbital contributions to the SIE, the dependence of the SIE on the separation distance between the dissociation fragments, and its impact on the equilibrium properties of **2–6**. A local analysis of the SIE in terms of exact and DFT exchange holes reveals that the SIE mimics not only non-dynamic but also an increasing amount of dynamic electron correlation effects as the number of valence electrons is enlarged. Standard DFT describes the dissociation of three-electron bonds qualitatively incorrectly. This can be traced back in the first instance to the SIE of the bonding β electron, which mimics a spurious long-range correlation with a non-existing delocalized α electron in the same bond. A comparison of the covalent (symmetric) and ionic (symmetry-broken) state of radical cations **2–6** at large interaction distances provides further insight in the inconsistencies of the DFT description: (i) Not only the SIE but also the approximate description of the interelectronic exchange contributes to the incorrect description of the dissociation. (ii) Dissociating three-electron bonds show a specific form of long-range correlation effects, which is neither accounted for by standard DFT, SIC-DFT nor Hartree–Fock theory. Indeed, SIC-DFT provides a qualitatively better description of the dissociation of radical cations, however in general a poor performance when describing equilibrium properties. There is no need for SIC-DFT methods. Instead, there is need for XC functionals with exact exchange and long-range correlation effects (*e.g.* mimicked by the exchange SIE) absorbed in the correlation functional. Implications of our findings for the construction of new density functionals are discussed.

1. Introduction

The development of improved exchange-correlation (XC) functionals for Kohn–Sham (KS) density functional theory (DFT)[1,2] has to consider the self-interaction error (SIE) of approximate X- and C-functionals.[3,4] In recent work, we have described the consequences and the impact of the SIE on a DFT description of molecules both in their equilibrium geometry and in the situation of bond breaking.[5–11] For this purpose, we have developed as descriptive tools an energy decomposition analysis based on the Perdew–Zunger approach[3] for self-interaction corrected DFT (SIC-DFT),[5] the difference density analysis reflecting the impact of the SIE,[5–7] and a decomposition analysis of the exchange hole, which makes it possible to relate the SIE to the correlation effects described in standard KS DFT.[8–10] Our work is in line with many investigations focusing on the SIE,[12–27] which had their forerunners already in the thirties in the work of Fermi and Amaldi[28] and in the fifties.[29] Our investigations revealed that the SIE of approximate X functionals accounts for non-specified short-range and long-range electron correlation effects, which can improve results of a standard DFT calculation and in general increase the stability of the KS-DFT solutions. This was also found or anticipated by authors such as Slater[29] (in connection with the discussion of charge transfer complexes), Becke[30] (when deriving the hybrid functionals) and in particular Baerends and co-workers who presented the first in detail discussion on this aspect of the SIE.[23] A quantification of the extra-correlation effects mimicked especially by the X-functional was possible by the combination of SIC-DFT calculations with difference density and exchange hole studies carried out in our previous work.[5–10]

The ambivalent role of the SIE, namely being an error and at the same time mimicking useful correlation effects, has to be considered when correcting standard DFT: SIC-DFT is not necessarily a better and more accurate method than standard DFT. On the other hand, SIC-DFT seems to be unavoidable if odd electron systems are investigated.[31–40] It is well known that standard DFT leads to an erroneous description of the dissociation of radical cations. For example, standard DFT predicts for the dissociation of H_2^+ an artificial transition state and a dissociation limit being just 14 kcal mol^{-1} above the equilibrium energy. Similar failures have been reported for the dissociation of other radical cations.[31–40] Consequently, much effort has been focused on the development of SIE-free DFT methods, which was either based on the Perdew–Zunger approach[3] or the idea to mix in exact exchange any time a large SIE is indicated by a suitable antenna as for example the von Weizsäcker kinetic energy density.[41,42]

In this work, we will show that SIE-free DFT leads to a number of new problems, which in general deteriorate the performance of DFT. For this purpose, we will investigate radical cations with three-electron bonds, which are known to present the most drastic SIE problems in DFT. We will describe these systems with different XC functionals ranging from the local density approximation (LDA) to modern hybrid functional theory and using both standard DFT and SIC-DFT. The accuracy of the various methods will be tested against experimental data (if available) or high level *ab initio* calculations. The calculated SIEs will be first decomposed in a pure electronic effect

DOI: 10.1039/b311840a

and an orbital relaxation effect and then into orbital contributions to identify orbitals with the strongest SIE. We will investigate exchange holes and by determining various contributions to the exchange hole identify those effects that lead to a deterioration of the DFT description. In particular we will answer the following questions.

(1) Does the SIE lead to systematic errors in calculated equilibrium properties of radical cations with three-electron bonds? Can they be quantified? Can one eliminate these errors for the radical cations? Or do other errors of standard DFT play a similarly important role so that a correct description of the radical cations is also not possible with SIC-DFT?

(2) How does the SIE influence the dissociation curves of radical cations with three-electron bonds? Is the electronic or the orbital relaxation effect of the SIE the main reason for the poor DFT description of the dissociation curves? Can SIE-free DFT improve the description of the dissociating radical cations?

(3) What is the correct description of the dissociation limit? Is it ionic (separation into a radical cation and a closed shell system) or is it covalent (separation into two fragments with charge and spin of 1/2 each)? Which DFT method gets closest to the correct description? How does the SIE of the fragments affect the results?

(4) What long-range correlation effects (if any) play an important role for the dissociation? Can standard DFT or SIC-DFT account for these effects?

(5) What conclusions can be drawn for the performance of standard DFT and SIC-DFT, for example for the description of radicals in general, transition states in radical or biradical reactions, or charge transfer complexes?

(6) What conclusions can be drawn for the development of new XC functionals? Is it desirable to use SIE-free XC functionals or do we have to change the strategy for the development of new XC functionals?

We will discuss these questions after a short description of the theory of the SIE and the SIC-DFT method used in this work (Section 2). Our discussion will be based on six different radical cations where we have included the $H_2^{+\bullet}$ (**1**) radical cation, which possesses just a one-electron bond, as a reference. The radical cations with a three-electron bond will be $He_2^{+\bullet}$ (**2**), $N_2H_6^{+\bullet}$ (**3**), $O_2H_4^{+\bullet}$ (**4**), $F_2H_2^{+\bullet}$ (**5**), and $Ne_2^{+\bullet}$ (**6**). These molecules can be considered as representatives for a large class of systems with odd-electron bonds. There will be enough evidence resulting from the discussion of the SIE accompanying the description of radical cations **1** to **6** for a balanced discussion of SIE-free XC functionals and their use in DFT. A strategy for the further development of XC correlation functionals will be derived in Section 4.

2. Computational methods

Coulomb interaction, exchange, and correlation occur between different electrons in a system. Hence, in a one-electron system, the correlation energy E_C must vanish, and the exchange energy E_X must exactly cancel the Coulomb energy J of the one electron. For any α-spin density ϱ_α that integrates to one, the following relations must hold:[3]

$$E_X[\varrho_\alpha, 0] = -J[\varrho_\alpha], \tag{1a}$$

$$E_C[\varrho_\alpha, 0] = 0. \tag{1b}$$

None of the commonly used approximate XC functionals obeys both eqns. (1a,b), *i.e.*, these XC functionals predict an unphysical self-interaction of the electrons. The construction of XC functionals that avoid this SIE intrinsically is difficult. Perdew and Zunger[3] suggested an expression for the XC energy that cancels the SIE orbital by orbital. The XC energy for the SIC-DFT formalism takes then the following form

$$E_{XC}^{\text{correct}} = E_{XC}^{\text{approx}}[\varrho_\alpha, \varrho_\beta] - E_{XC}^{\text{SIE}}, \tag{2a}$$

$$E_{XC}^{\text{SIE}} = E_X^{\text{SIE}} + E_C^{\text{SIE}}, \tag{2b}$$

$$E_X^{\text{SIE}} = \sum_{\sigma=\alpha,\beta} \sum_{i=1}^{N_\sigma} (E_X[\varrho_{i\sigma}, 0] + J[\varrho_{i\sigma}]), \tag{2c}$$

$$E_C^{\text{SIE}} = \sum_{\sigma=\alpha,\beta} \sum_{i=1}^{N_\sigma} E_C[\varrho_{i\sigma}, 0], \tag{2d}$$

where $\varrho_{i\sigma}(\boldsymbol{r}) = |\varphi_{i\sigma}(\boldsymbol{r})|^2$ is the density that corresponds to the KS spin orbital $\varphi_{i\sigma}$.

The SIC-DFT-KS equations differ from the standard-KS equations in two ways: (a) The KS operator $\hat{F}$ contains an additional orbital-dependent term that accounts for the correction of the SIE. (b) Orbital rotations between the occupied orbitals affect the total energy, and one is no longer free to choose the representation of the occupied KS orbitals (*i.e.* canonical or localized), instead this choice is a part of the energy optimization. As a rule, the resulting KS orbitals are localized.[13]

Solving the SIC-DFT-KS equations self-consistently (SC) is by far more expensive than a standard KS-DFT calculation. A reasonable approximation to SC-SIC-DFT is to abandon self-consistency and to calculate the SIC perturbatively for the orbitals resulting from a standard KS calculation. A subtle point in the perturbative (P) SIC-DFT scheme is the appropriate choice of the orbitals for the calculation of the SIC. SC-SIC-DFT yields localized orbitals in most cases, hence, a reasonable approach is to localize the occupied KS orbitals, *e.g.* according to the Foster–Boys criterion[43] before obtaining the P-SIC-DFT results. P-SIC-DFT allows assessment of the impact of the SIE at a computational cost comparable to a standard KS-DFT calculation. Furthermore, the combination of P-SIC-DFT and SC-SIC-DFT as done in this work makes it possible to separate the pure electronic and the orbital relaxation effect of SIE, which are oppositely directed in most cases. Both SC-SIC-DFT and P-SIC-DFT were implemented in the program package COLOGNE 2003.[44] The details of the implementation are described elsewhere.[11]

Special care has to be taken with the P-SIC-BLYP calculations for radical cations such as **6**. A simultaneous localization of all valence orbitals leads to instabilities in the localization procedure, resulting in fluctuations of the total energies by about 0.2 kcal mol^{-1}, which make a geometry optimization impossible. Therefore, the orbitals of **6** were localized in three groups: (i) the 1s orbitals, (ii) the 2s and 2p σ orbitals, and (iii) the 2p π orbitals. This required in turn a consistent description of the Ne atom and the Ne^+ ion. The localization of orbital group (ii) in **6** leads to two spσ orbitals (half-bond and lone pair) at each Ne atom. For β spin, one obtains a bond orbital, which has predominantly pπ character, and a localized s orbital at each Ne atom. Therefore, in the Ne atom a localization was done for the 2s and one of the 2p orbitals for α spin whereas the canonical orbitals were used for β spin. For the Ne^+ ion, canonical orbitals were used throughout.

For radical cations **2**, **3**, **4**, **5**, and **6**, we calculated dissociation curves with a number of pure and hybrid XC functionals that combine different mixtures of the Becke 88 exchange[45] and exact exchange with the Lee-Yang-Parr (LYP) functional:[46] the BLYP functional[45,46] with the portion a_{HF} of exact exchange being 0, the B3LYP functional[46,47] with $a_{HF} = 0.2$, the BH&HLYP functional[46,48] with $a_{HF} = 0.5$, and the HFLYP[46] functional, which combines exact exchange with LYP correlation, *i.e.*, $a_{HF} = 1$. HFLYP is the most common representative for the so-called HF-KS schemes, which combine HF exchange with a DFT correlation functional. As the LYP correlation functional contains no self-interaction,

the HFLYP functional is SIE-free by construction. The distance $R(X–X) = R$ between the two atomic or molecular fragments was used as the dissociation parameter. The geometries of **3** to **5** were optimized for a number of points along the dissociation curve with the given value of R frozen. As a reference we calculated the dissociation curves with CCSD(T).[49] For the purpose of studying the impact of self-interaction corrections on the result, we recalculated the BLYP dissociation curves both with P-SIC and with SC-SIC. For all dissociation curves, Dunning's cc-pVTZ basis set[50] was used except for the SC-SIC calculations where we had to resort to the cc-pVDZ basis set[50] to ensure convergence. For **10**, **2**, and **6**, we calculated in addition the orbital contributions to the SIE in dependence of R for P-SIC-BLYP and the cc-pVTZ basis set.

Beside the BLYP and the BLYP related functionals, a number of other LDA and GGA (generalized gradient approximation) XC functionals were used to determine the bond length r_e, the dissociation energies D_e, and the harmonic vibrational frequencies ω_e both with standard KS-DFT and with P-SIC-DFT employing cc-pVTZ basis set for **1**, **2**, and **6**: (1) SVWN,[51,52] (2) PW91PW91,[53] (3) BP86,[45,54] (4) BPW91,[45,53] (5) B3P86,[47,54] (6) B3PW91,[47] (7) mPW1PW91.[55]

As a basis for discussing differences between even-electron bonded and odd-electron bonded molecules, we additionally computed dissociation curves for neutral H_2 (**10**) at the BLYP, P-SIC-BLYP, and SC-SIC-BLYP levels of theory (SC-SIC-BLYP is actually equivalent to HFLYP for **1**), both spin-restricted and spin-unrestricted. As suitable reference, we calculated the dissociation curve with both spin-restricted and spin-unrestricted CISD[56] because CISD corresponds to full CI for a two-electron system. These calculations were all done with the cc-pVTZ basis set.[50]

For P-SIC and SC-SIC, the quantities r_e and D_e were determined by interpolating the calculated points on the dissociation curve with a cubic spline and calculating the minimum of this spline function because analytical gradients are currently not available for these methods. As for the impact of the SIE on the vibrational spectrum, we evaluated the harmonic adiabatic stretching frequencies $\omega_e^a(X–X)$[57] in the case of the polyatomic radical cations **3**, **4**, and **5**. Adiabatic vibrational modes are strictly localized at that internal coordinate that leads the adiabatic mode (*e.g.* the bond distance). The force constant of the adiabatic X–X stretching frequency gives the curvature of the dissociation curve at r_e and behaves in a similar way as the true harmonic vibrational frequency ω_e corresponding to X–X stretching. The latter however is delocalized and contains small contributions of the motions of other atoms.

For the purpose of investigating the existence and stability of covalent and ionic state, each of these states was calculated for **1**, **2**, and **6** at an interaction distance of 10 Å with the four DFT functionals mentioned above, additionally with HF and SC-SIC-BLYP. Stability tests[58,59] were performed for all methods except SC-SIC. The geometries were prepared in the following ways: For the ionic states, we started from the geometries of the neutral and ionic fragments, *i.e.* NH_3 (**7**) and $NH_3^{+\bullet}$ ($\mathbf{7}^{+\bullet}$) for **3**, OH_2 (**8**) and $OH_2^{+\bullet}$ ($\mathbf{8}^{+\bullet}$) for **4**, FH (**9**) and $FH^{+\bullet}$ ($\mathbf{9}^{+\bullet}$) for **5**, and assembled these fragments at a distance R of 10 Å between the heavy atoms using the appropriate symmetry (C_{3v} according to HNNH dihedral angles of 60° for **3**, C_σ according to the anti form of **4**, and $C_{\infty v}$ for the linear arrangement of the fragments in **5**). Radical cation **4** is more stable in the *gauche* conformation, which is true at all levels of theory used in this work. For the purpose of simplifying the analysis of the SIE in this case the C_2-symmetric anti form was used throughout this work. In Scheme 1, all molecules and their conformations are shown.

All SIC-DFT calculations were carried out with the Cologne 2003 program package,[44] CCSD(T) calculations with the ACES II program package,[60] and standard DFT calculations with the Gaussian 98 program package.[61] COLOGNE 2003 contains also program routines for the calculation of exchange holes and their presentation in the form of one- or two-dimensional diagrams.[8–11]

3. Results and discussion

In Tables 1, 2, and 3, the calculated properties (X–X bond lengths r_e, X–X dissociation energies D_e, and harmonic X–X stretching frequencies ω_e) for diatomic radical cations **1**, **2**, and **6** are summarized. For the polyatomic radical cations **3**, **4**, and **5**, these properties are listed in Table 4. Calculated dissociation curves are shown in Fig. 1 (**1**, **2**, and **6**) and Fig. 2 (**3**, **4**, and **5**). We will first discuss the calculated properties of the diatomic radical cations, and then those of the polyatomic radical cations.

3.1 Properties of radical cations with three-electron bonds

Standard DFT gives a slight (about 3–5 kcal mol^{-1}) overbinding of **1** and a strong overbinding of **2** (15 kcal mol^{-1} for LDA) and **6** (43.5 kcal mol^{-1} for LDA). For **1**, the LDA value is in the interval spanned by the GGA values; for **2** and even more so for **6**, LDA gives a stronger overbinding than GGA. P-SIC-GGA calculations underestimate the dissociation energies of **2** by up to 9 kcal mol^{-1}, whereas P-SIC-LDA calculations slightly (5 kcal mol^{-1}) overestimates this dissociation energy. Equally as for the bond lengths, mixing in an increasing portion of exact exchange reduces the overbinding as well as the differences between standard-DFT and P-SIC-DFT values. The P-SIC-DFT values are less dependent on the choice of the XC functional, both with respect to the approximation used and the introduction of hybrid exchange, than the standard-DFT ones.

It is important to note that the D_e value for three-electron-bonded systems decreases strongly with a_{HF}. This can also be seen from Figs. 1 and 2 to an increasing extent when comparing dissociation for **3**, **4**, **5**, and **6**. For one-electron-bonded systems, D_e is much less sensitive to a_{HF}, as can be seen from the results for **1** (see also ref. 11).

Similar trends can be found for the calculated bond lengths and harmonic frequencies. Since these properties have been partially discussed in the previous literature, we refrain from discussing them here.

Dissociation curves of radical cations with three electrons. Figs. 1 and 2 show the X–X dissociation curves for **2** to **6** for BLYP, B3LYP, BH&HLYP, HFLYP, SC-SIC-BLYP, P-SIC-BLYP, and CCSD(T). The standard-DFT calculations show a qualitatively incorrect dissociation behavior: For the separation distance R increasing from the equilibrium bond length, the energy does not increase monotonically to zero but possesses a maximum for a finite R, beyond which it predicts a Coulomb repulsion between the fragments and a negative limit energy, *i.e.*, for increasing R the molecule passes an artificial transition state. The smaller a_{HF} is, the lower is the energy of this transition state, the stronger is the Coulomb repulsion, and the more negative is the relative energy (*i.e.*, the energy of the supermolecule minus the energy of the fragments) for $R \rightarrow \infty$. HFLYP (*i.e.* $a_{HF} = 1$) gives a qualitatively correct dissociation behavior. It is interesting to note that for **2** the HFLYP dissociation curve is close to the CCSD(T) reference curve, while HFLYP seriously underestimates D_e for **3–6**.

SC-SIC-DFT leads to the correct dissociation behavior and a reasonable overall agreement with the CCSD(T) reference. However, the SC-SIC-DFT and CCSD(T) curves approach their limit for $R \rightarrow \infty$ in different ways: The CCSD(T) curve leads smoothly to the limit of a vanishing relative energy for $R \rightarrow \infty$. The SC-SIC-DFT dissociation curve, in contrast,

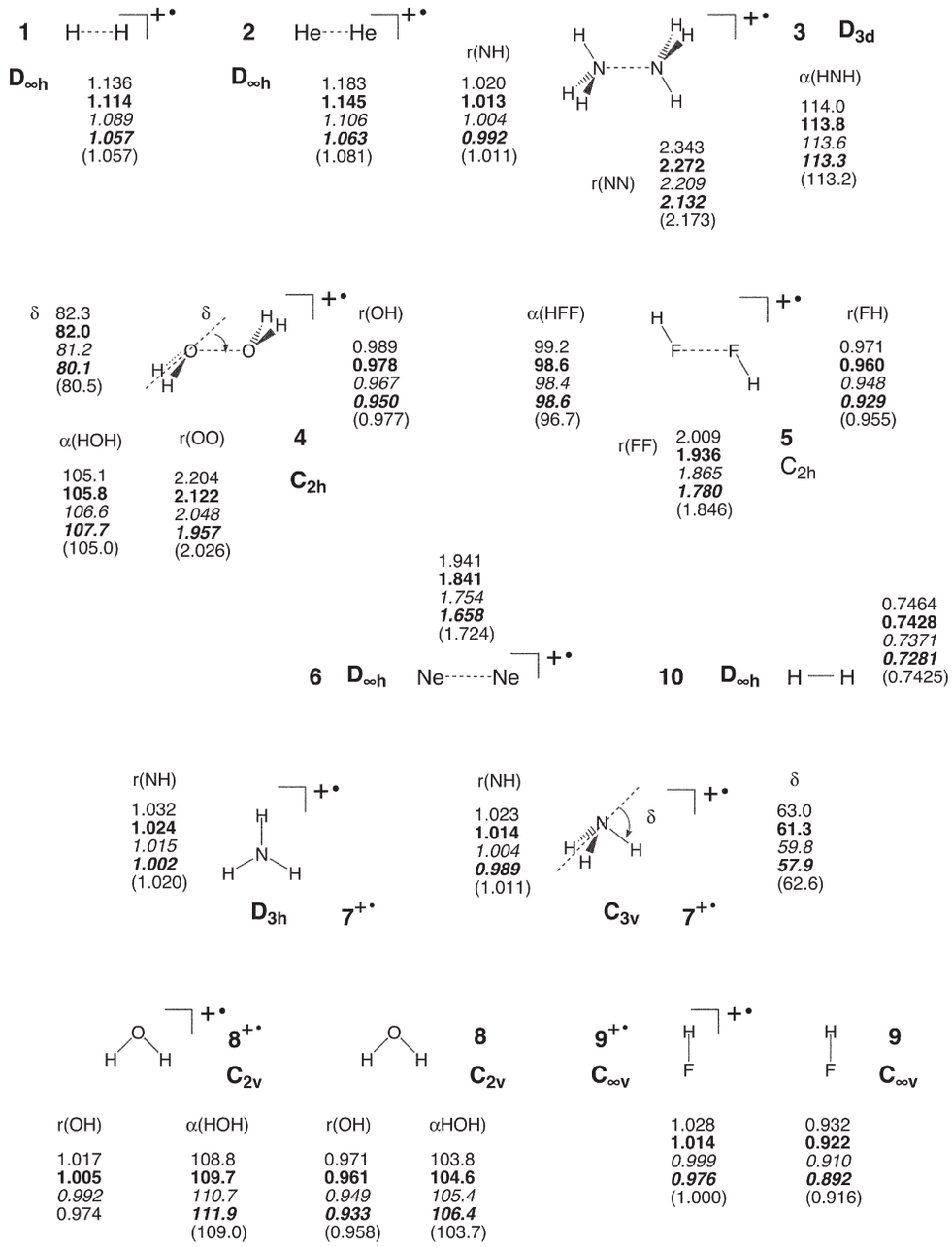

Scheme 1 The molecules investigated in this paper and their geometries. Plain typeface: BLYP, boldface: B3LYP, italic: BH&HLYP, italic boldface: HFLYP, values in parentheses: CISD for **10**, CCSD(T) otherwise. SC-SIC-DFT calculations done with Dunning's cc-pVDZ basis set,[50] all other calculations with Dunning's cc-pVTZ basis set.[50]

shows a rapid increase of the energy for R slightly above r_e and then continues nearly horizontally to the limit value. An analysis of the SC-SIC-DFT solutions shows that this abrupt change of the slope is an indication of a symmetry breaking: For small R the solution corresponds to the covalent state of the molecule. Above a certain R value, the covalent solution rearranges into the symmetry-broken (ionic) one where the positive charge and the spin are more and more concentrated on one fragment as R increases. The covalent solution still exists but is unstable.

The same kind of symmetry breaking occurs also for the HFLYP solution. This has been illustrated for **6** where the HFLYP dissociation curve is shown both for the covalent and the ionic state. The ionic solution shows an even more abrupt change in the slope than the SC-SIC-DFT curve. The curve for the covalent state, in contrast, is smooth but predicts a negative relative energy of the supermolecule at large R. P-SIC-DFT, in contrast to SC-SIC-DFT, yields a positive relative energy for $R \rightarrow \infty$. However, it avoids the artificial transition state and leads to smaller deviations from the CCSD(T) reference than standard DFT. HFLYP and P-SIC, and to a lesser extent SC-SIC-DFT, systematically underestimate D_e and tend to give too short bond lengths.

In addition to the dissociation curves, Figs. 1 and 2 show the SIE for the relative energies, *i.e.* the SIE of the molecule minus the SIEs of the fragments both at the P-SIC (P-SIE) and the SC-SIC (SC-SIE) level of theory for the Becke88 exchange functional. For R values close to r_e and above the SIE is a monotonically decaying, convex function of R. For smaller R values, the SIE shows an inflection point and becomes a concave function of R. For **4** and **5**, P-SIE-B = f(R) has an extremum and becomes monotonically increasing for small R; for SC-SIE-B, this behavior was not found. In all cases, both the P-SIE and the SC-SIE correction of the dissociation energies are negative for all values of R. The SC-SIE correction is generally more positive, *i.e.* its magnitude is smaller than that

Table 1 Calculated equilibrium bond lengths for radical cations $H_2^{+\bullet}$ (**1**), $He_2^{+\bullet}$ (**2**), and $Ne_2^{+\bullet}$ (**6**)[a]

	1		2		6	
Method	Std.	P-SIC	Std.	P-SIC	Std.	P-SIC
SVWN	1.153	1.054	1.159	1.045	1.823	1.601
BP86	1.134	1.050	1.175	1.056	1.939	1.657
BLYP	1.136	1.048	1.183	1.057	1.941	1.658
PW91PW91	1.130	1.050	1.173	1.050	1.927	1.635
BPW91	1.127	1.049	1.177	1.056	1.966	1.656
mPW91PW91	1.105	1.053	1.130	1.055	1.821	1.647
B3P86	1.110	1.053	1.135	1.057	1.829	1.655
B3LYP	1.114	1.052	1.145	1.058	1.841	1.657
B3PW91	1.110	1.052	1.139	1.057	1.844	1.655
BH&HLYP	1.090	1.055	1.105	1.060	1.754	1.660
HFLYP	1.057	1.057	1.063	1.063	1.658	1.658
lh-BLYP[b]	1.06		1.06		1.79	
HF	1.057		1.075		1.697[c]	
					1.877[d]	
CCSD(T)	1.057		1.081		1.721[c]	
					1.712[d]	
Experiment	1.052[e]		1.081[e]			

[a] Bond lengths given in Å. Abbreviations Std. and P-SIC denote standard Kohn–Sham DFT and perturbative SIC-DFT calculations. Dunning's cc-pvtz basis set[50] was used. [b] From ref. 42. [c] Covalent state. [d] Ionic state. [e] From K. P. Huber and G. Herzberg, *Constants of Diatomic Molecules*, Van Nostrand Reinhold, New York, 1979.

Table 3 Harmonic vibration frequencies for radical cations $H_2^{+\bullet}$ (**1**), $He_2^{+\bullet}$ (**2**), and $Ne_2^{+\bullet}$ (**6**)[a]

	1		2		6	
Method	Std.	P-SIC	Std.	P-SIC	Std.	P-SIC
SVWN	1879.7	2354.6	1311.5	1881.9	392.4	860.0
BP86	1913.9	2380.0	1219.3	1843.7	274.4	766.8
BLYP	1880.8	2395.5	1195.2	1846.8	304.7	775.7
PW91PW91	1919.0	2382.4	1223.1	1869.1	287.3	807.1
BPW91	1929.3	2387.7	1204.5	1845.2	245.6	770.4
mPW1PW91	2053.9	2360.0	1421.9	1840.7	411.3	777.8
B3P86	2038.2	2361.6	1397.9	1831.3	398.8	768.3
B3LYP	2002.8	2369.9	1367.1	1833.1	351.3	771.2
B3PW91	2030.2	2364.8	1379.4	1831.1	380.5	766.6
BH&HLYP	2139.5	2348.4	1562.6	1820.7	404.6	761.0
HFLYP	2334.4	2373.7	1818.7	1818.7	476.8	677.5
HF	2334.4		1746.1		616.1[b]	
					160.8[c]	
CCSD(T)	2334.4		1705.9		577.9[b]	
					606.5[c]	
Experiment	2324.7[d]		1698.5[d]			

[a] Frequencies are given in cm^{-1}. Abbreviations Std. and P-SIC denote standard Kohn–Sham DFT and perturbative SIC-DFT calculations. Dunning's cc-pVTZ basis set 50 was used. [b] Covalent state. [c] Ionic state. [d] From K.P. Huber and G. Herzberg, *Constants of Diatomic Molecules*, Van Nostrand Reinhold, New York, 1979.

of P-SIE. Hence, the electronic effect included by the P-SIC-DFT approach gives an exaggerated SIE correction for $D_e(R)$, whereas the orbital relaxation correction reduces this. Both the electronic and the orbital relaxation SIE are larger for the radical cation than the fragments. P-SIE is a positive destabilizing correction because stabilizing correlation effects (see below) mimicked by the SIE are deleted. The difference in the SIEs of the fragments and the molecule grows with increasing R and since the latter SIE is deducted from the former SIEs, the P-SIE becomes increasingly negative. The orbital relaxation effects are negative (stabilizing) so that the correction for the relative energies becomes positive. The total SIE converges to a value given by the BLYP dissociation curve for large R (Figs. 1 and 2).

Table 2 Dissociation energies D_e for radical cations $H_2^{+\bullet}$ (**1**), $He_2^{+\bullet}$ (**2**), and $Ne_2^{+\bullet}$ (**6**)[a]

	1		2		6	
Method	Std.	P-SIC	Std.	P-SIC	Std.	P-SIC
SVWN	67.04	64.37	84.92	61.19	83.53	54.99
BP86	69.11	63.86	82.50	52.96	73.61	37.17
BLYP	69.08	63.65	83.30	53.49	75.41	37.73
PW91PW91	68.90	63.75	78.52	51.14	75.74	44.16
BPW91	69.72	63.70	78.35	48.46	72.43	35.39
mPW1PW91	67.98	63.99	70.96	51.23	55.04	33.97
B3P86	68.09	64.02	76.82	54.87	59.27	34.19
B3LYP	67.83	63.93	77.38	55.31	60.54	34.45
B3PW91	68.35	63.96	73.56	51.44	58.10	32.54
BH&HLYP	66.36	64.15	69.14	56.36	39.99	26.16
HFLYP	64.28	64.28	57.86	57.86	11.32	11.32
lh-BLYP[b]	64.3		54.9		33.9	
HF	64.28		45.41		2.78[c]	
					3.18[d]	
CCSD(T)	64.28		56.04		30.87[c]	
					30.80[d]	
Experiment	64.39[e]		56.94[e]			

[a] Relative energies given in kcal/mol. Abbreviations Std. and P-SIC denote standard Kohn–Sham DFT and perturbative SIC-DFT calculations. Dunning's cc-pvtz basis set[50] was used. [b] From Ref. 42. [c] Covalent state. [d] Ionic state. [e] From K.P. Huber and G. Herzberg, *Constants of Diatomic Molecules*, Van Nostrand Reinhold, New York, 1979. The D_e value has been calculated from the experimental D_0 and ω values.

3.2 The SIE for three-electron bonds

The SIE of the bonding electron was investigated for one-electron-bonded radical cations using a simple estimate for the SIE of the bond orbital dominating the whole error for increasing R.[12,36]

$$E^{\mathrm{SIE}} = (1-\alpha_{\mathrm{HF}})\left[\underbrace{\left(\frac{1}{2}-C\right)}_{<0}J+\frac{1}{4R}\right]. \qquad (3)$$

Here, $C \approx 2^{-1/3}$, $(0.5-C) \approx -0.79$, and J is the Coulomb self-interaction for the case that the bond electron is localized at either of the two fragments. Estimate (3) reflects (i) the negative sign of the SIE and by this the strong reduction of the relative energies for $R \to \infty$, (ii) the Coulomb decrease of the dissociation energy (the artificial Coulomb potential in (3) decreases for increasing R), and (iii) the decrease of the SIE with increasing a_{HF}. The question arises whether estimate (3) may be used in the case of three-electron bonds as well. This is indeed the case: the three-electron bond may be built from a triplet state with one α electron in the bonding and antibonding orbital each by adding a β electron to the bonding orbital. If only the α electrons are present, there is exchange repulsion between the two fragments for small R and no bonding otherwise. (We ignore the Coulomb repulsion between the two positively charged fragments as it will be reduced by the screening effect of the β electron.) Both the bonding and the antibonding orbital are occupied, and the two α electrons may be treated either as localized or delocalized. In the calculation of the SIE, the electrons are to be treated as localized, and consequently the SIE of the two α electrons is small, in particular

Table 4 Dissociation energies, equilibrium bond lengths, and harmonic vibrational frequencies for radical cations **3**, **4**, and **5**[a]

	3				4				5			
	D_e	r_e	ω_e	ω_e^a	D_e	r_e	ω_e	ω_e^a	D_e	r_e	ω_e	ω_e^a
BLYP	48.55	2.343	304.7	421	59.93	2.204	317.1	657	68.80	2.009	345.0	686
B3LYP	44.21	2.272	351.3	664	52.43	2.122	381.0	635	58.50	1.936	419.0	658
BH&HLYP	37.46	2.209	404.6	671	41.64	2.048	450.7	953	43.76	1.865	503.5	1067
HFLYP	29.16	2.132	476.8	580	27.76	1.957	548.3	853	23.83	1.780	623.0	991
P-SIC-BLYP	39.00[c]	2.176		750	32.26	2.005		1011	31.71	1.816		1142
SC-SIC-BLYP	39.19[c]	2.193		1644	40.91	2.050		1508	38.69	1.866		1192
lh-BLYP[d]	39.8	2.25			35.5	2.08			38.6	1.90		
CCSD(T)	36.34	2.173		1634	40.75	2.026		1414	40.22	1.846		1036

[a] P-SIC-BLYP calculations at BLYP geometries, SC-SIC-BLYP calculations at CCSD(T) geometries. SC-SIC calculations done with Dunning's cc-pVDZ basis set,[50] all other calculations with Dunning's cc-pVTZ basis set.[50] Energies in kcal mol^{-1}, bond distances in Å, frequencies in cm^{-1}. The ω_e values shown are for the N–N, O–O, and F–F stretching vibrations, respectively. For an explanation of the adiabatic frequencies ω_e^a, see Section 3. [b] From K. P. Huber and G. Herzberg, *Constants of Diatomic Molecules*, Van Nostrand Reinhold, New York, 1979. The D_e value has been calculated from the experimental D_0 and ω_e value. [c] According to SIC-BLYP calculations, **7'** is pyramidal. This leads to D_e values of 33.8 and 32.8 kcal mol^{-1} at the P-SIC-BLYP and SC-SIC-BLYP levels of theory. [d] From ref. 42.

if a GGA functional is used, since the SIE decreases (increases) with growing localization (delocalization). It depends only weakly on R (except for very small R where exchange repulsion is sizable). The bonding between the fragments is accomplished by the delocalized β electron. This electron dominates the total SIE, and consequently, the estimate from the one-electron cases remains valid. This is confirmed by inspection of the orbital contributions to the SIE and the analysis of the exchange holes.

Orbital contributions to the SIE. The orbital contributions to the SIE are shown in Fig. 3 for **1** (Fig. 3a), **2** (Fig. 3b), and **6** (Fig. 3c). In the case of **1** the SIE of the H atom is given as a reference. The SIE of the paired electrons in **6** and that of the two α electrons in **2** is independent of R except for small R values where the exchange repulsion between the fragments plays a role. The SIE for the bonding β orbital is absolutely larger than that of the other orbitals and decreases according to a Coulomb-law term. The sign of the SIE for the localized orbitals varies: Whereas the SIE for the 1s orbital of **2** is close to zero, for **6** the SIE is positive for the 1s orbitals and negative for the localized 2sp orbitals. Becke 88 exchange[45] is constructed such that the total SIE is small for a compact rotationally symmetric charge distribution. For an isolated He^+ ion, the SIE of the Becke 88 exchange functional should thus nearly vanish, which is reflected by the small absolute value of the SIE. For the Ne^+ ion, the SIE does not vanish orbital by orbital, rather there is a compensation between the positive SIE for the compact 1s orbitals and the negative SIE for the more diffuse 2s and 2p orbitals.

Eqn. (3) explains the errors in the DFT values for r_e, D_e, and ω_e found for **1** and the three-electron-bonded systems **2** to **6**. The dominating contribution to the SIE is monotonically decreasing, except possibly for R values well below r_e. Consequently, the SIE shifts the energy minimum of the dissociation curve towards a larger R value. The negative sign of the SIE accounts for the overestimation of D_e. The underestimation of the ω_e is at a first glance surprising. The SIE is a convex function of R at $R = r_e$ for **1**, **2**, and **6** and should thus increase the force constant and eventually ω_e. However, the second derivative of the energy with respect to R decreases with increasing R, and the overestimation of r_e mentioned above eventually results in an underestimation of ω_e.

LDA overestimates r_e more strongly than GGA for **1**, while the situation is *vice versa* in **2** and **6**. This can be understood from the orbital contributions to the SIE. For **1**, only the SIE of the bonding electron is present, which influences r_e more strongly for LDA than for GGA. For **2** and **6**, the SIE of the localized orbitals increases weakly with R, thus tending to decrease r_e. GGA has very small SIE's for localized orbitals, and the shortening of the bond length is negligible. For LDA in contrast, the SIE of the localized orbitals is larger, and the overestimation of R caused by the SIE of the bond electron is partly compensated.

Analysis of the SIE with the help of the exchange hole. In Figs. 4 and 5, exchange holes of the bonding β electron of **2** and **6** are shown as calculated for different internuclear distances, different positions (P1 or P2) of the reference electron, and for different methods. For both molecules the holes have been calculated for the bonding β electron because there the largest differences can be observed. For the two α electrons of the three-electron bond the HF and GGA hole do not differ very much. Both are localized for the reference electron being at one of the nuclei and they vanish for the reference electron at the bond center P1. For the purpose of analyzing the form of the various exchange holes, it is useful to outline some relationships.

(a) The exchange hole can be split into an intraelectronic (self-exchange) and interelectronic part. The magnitude of each part depends on the orbitals used. If one uses localized orbitals, the intraelectronic part is maximized. The intraelectronic exchange hole fulfills the sum rule (integration leads to −1), which means that integration over the interelectronic exchange hole leads to zero.

(b) The SIE part of the DFT exchange hole can be evaluated as the difference between the DFT and the SIC-DFT hole. Since in this work the same density is used for the description of the HF, DFT, and SIC-DFT hole to facilitate the comparison, the SIC-DFT and the HF exchange hole are identical for one electron. In this case the SIE hole results from the difference between the DFT and HF holes. In general, the SIE hole is the difference between the intraelectronic DFT and the intraelectronic SIC-DFT hole because their interelectronic exchange holes are identical.

(c) If the reference electron is in the middle of the X–X bond at P1, interelectronic HF and GGA exchange are vanishingly small and the exchange holes are equal to the intraelectronic exchange parts. Also, the reduced gradient is equal to zero so that the GGA hole is identical to the LDA exchange hole. Since the same density is used for the representation of the exchange hole, all holes must have the same value at the position of the reference electron.

(d) SIE hole and SIE energy are related *via* the electron density. The SIE part of a DFT exchange hole can be rather large, however if the density is very small at the position of the reference

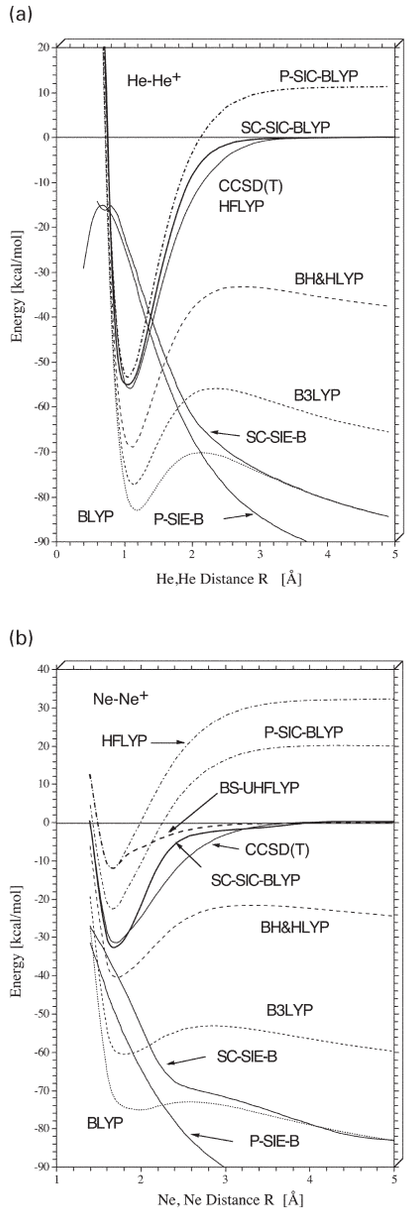

Fig. 1 Dissociation curves for He_2^+ (a) and Ne_2^+ (b) calculated with DFT and wave-function methods are shown. The SIE obtained with P-SIC-BLYP (P-SIE-B) and SC-SIC-BLYP (SC-SIE-B) is given relative to the SIEs of the fragments. In Fig. 1b, both the symmetry-adapted (covalent) and symmetry-broken (ionic) solution for HFLYP are shown. Dunning's cc-pVTZ basis set[50] was used for all calculations.

electron the large SIE hole will not have any effect on the SIE energy.

If the reference electron is at the center of the He–He bond (position P1, Fig. 4a), the HF exchange hole is symmetric, delocalized, and equal to the negative electron density distribution of the β electron. The local GGA exchange hole possesses at P1 the same value as the HF hole (provided the same density is used). Otherwise it is rather flat, spherical, and centered at P1. The difference between the two holes gives the SIE part of the GGA hole because both the HF hole and the GGA exchange holes are equal to their intraelectronic part and, in addition, the HF hole is equal to the SIC-GGA hole. The SIE accounts for a large portion of the GGA hole and converts the localized GGA hole into the delocalized SIC-GGA hole. If the reference electron is at P1, a fictitious second electron is found with the same probability at either He1 or He2 (Fig. 4a). Hence, a non-dynamic correlation effect is simulated, which is not needed. Nevertheless, it artificially stabilizes the radical cation of the DFT description. With increasing R, the SIE and by this the non-dynamic correlation effect increases since the separation between the maximum probabilities for the fictitious second electron is also increased.

If the β-electron is at nucleus He2 (position P2 in Fig. 4b), the form of the HF exchange hole and also that of the SIC-GGA exchange hole does not change because the delocalized hole is static (*i.e.* independent of the position of the reference electron). A static exchange hole cannot describe any correlation effects. However, if the delocalized SIC-GGA hole is converted into a GGA hole localized close to position P2, this will be only possible by adding a large SIE part that depends on the position of P2 and describes again a long-range (non-dynamic) correlation effect. Again, this effect increases with increasing distance R.

We can relate the form of the SIE exchange hole to the formula for the SIE energy given in eqn. (3). For this purpose, we have to combine the hole with the electron density distribution. The SIE exchange hole can be considered as the difference of the DFT X hole minus the SIC-DFT X hole or, alternatively as the sum of the Coulomb self-repulsion and the DFT X hole. In the latter case, the first part leads to an electron distribution exactly opposite to the HF = SIC-DFT exchange hole, *i.e.* two densities integrating to $1/2$ unit charge each repel each other at the distance R thus yielding the artificial Coulomb potential $1/(4R)$. With increasing distance R the destabilizing Coulomb part vanishes. It remains the localized DFT exchange hole, which corresponds to an energy approximately equal to $(0.5 - C)J_A$, which is always negative and represents the limit of the SIE energy for $R \rightarrow \infty$. Hence, the connection between eqn. (3) and the form of the SIE part of the DFT exchange hole becomes obvious.

The exchange hole of the β-electron in the ionic state of **2** (Fig. 4c) is, contrary to the symmetry-adapted delocalized X hole, localized since the electron is now localized at one of the atoms. Consequently, UHF and UGGA exchange holes for the ionic state differ only in a limited way. The SIE of the GGA functional describes some dynamic short-range correlation where these effects are as unrealistic as the non-dynamic correlation effects mimicked by the the DFT X hole of the covalent state: A second electron does not exist and, therefore, there is no dynamic electron correlation of the β electron; however, the correlation error is now much smaller.

In the case of **6** the β electron experiences beside Coulomb correlation also interelectronic exchange with the other β electrons missing for **2**. In Fig. 5a, the situation of the exchange hole is shown for the reference electron being located at the midpoint of the bond (P1). At P1, the effect of the $3\sigma_g$ bonding orbital is dominant, but the effect of the two sp lone pairs of the Ne atoms transmitted *via* their tails is still significant. This explains the structure of the HF exchange hole, which is symmetric and resembles at the nuclei the corresponding exchange hole of **2**; the broadening of the hole in the nonbonding region is due to the sp lone pair orbitals. The SIC-DFT X hole has a similar structure, is however no longer identical to the HF exchange hole because of small deviations in the interelectronic exchange, which is zero for the GGA X hole but has a small finite value for HF exchange. The SIE part of the localized, spherically symmetric GGA hole is again large and mimics left–right long range (non-dynamic) electron correlation effects, which are not needed. They lead to an artificial stabilization of **6** for $R = 1$ Å. This stabilization is however partially compensated by Coulomb self-repulsion caused by the β electron so that the net effect is not large.

At 3.5 Å the situation changes significantly because there is at P1 only the influence of the delocalized β electron. The HF exchange hole takes a form that is reminiscent of two 2pσ orbitals localized at the atoms without any significant overlap in the bonding region so that the density at P1 is close to zero. The GGA hole localized at P1 is consequently so flat and shallow that it can no longer be distinguished from the zero line

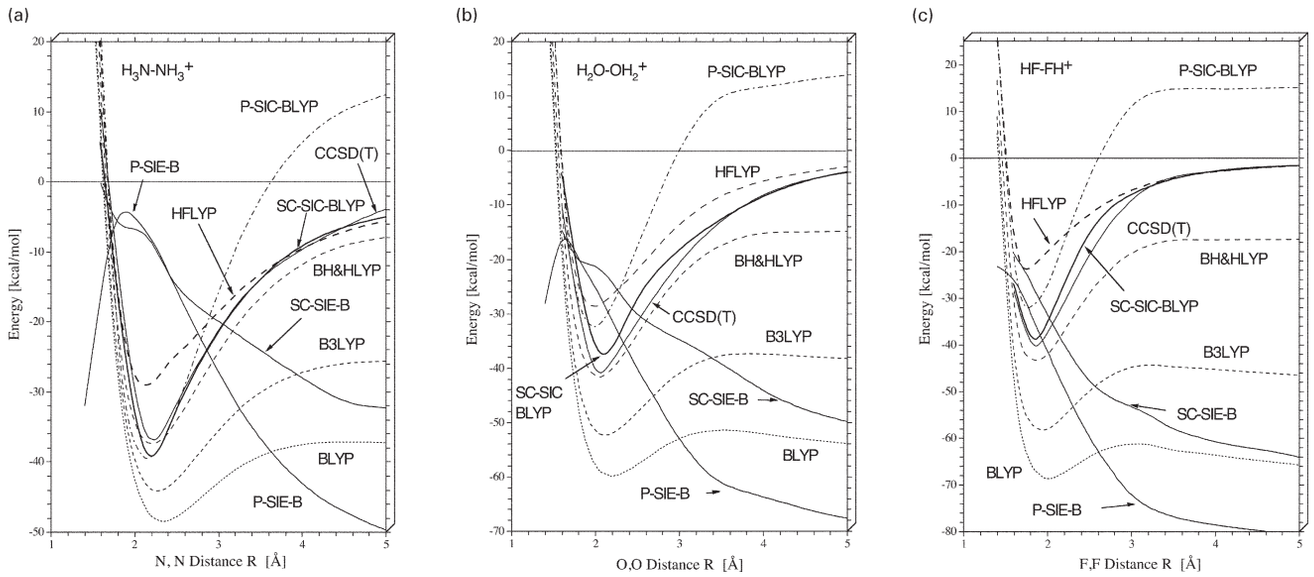

Fig. 2 Dissociation curves for radical cations $N_2H_6^+$ (a), $O_2H_4^+$ (b), and $F_2H_2^+$ (c) calculated with the DFT and wave-function methods are shown. The SIE obtained with P-SIC-BLYP (P-SIE-B) and SC-SIC-BLYP (SC-SIE-B) is given relative to the SIEs of the fragments. Dunning's cc-pVTZ basis set[50] was used for all calculations.

(Fig. 4a). HF and SIC-GGA hole are identical and accordingly, a strong SIE being the mirror image of the SIC-GGA (HF) hole is obtained. The energetic consequences of this SIE are nil because the electron density at P1 is negligible. We conclude that because of the low probability of the β electron being at the midpoint of the bond there is no longer a non-dynamic correlation effect. This will be recovered to some extent if the β electron moves closer to a particular Ne atom, *e.g.* to Ne2. The SIE part of the exchange hole has a similar form at Ne1 as shown in Fig. 5a whereas at Ne2, the SIE hole simulates now also strong short-range (dynamic) correlation effects.

If the β electron is located at nucleus Ne2 (position P2, Fig. 5b), the X hole becomes localized (contrary to what was found in the case of **2**; Fig. 4b). This is the result of contributions of the core electrons, which enter the formula for the dominating intraelectronic exchange hole by the factor ρ_i/ρ where ρ_i is the orbital density at P1 and ρ the total density at this point. The core electrons strongly reduce the influence of the β electron on the the form of the X hole so that the localization of the exchange hole results (insert in Fig. 5b). HF and GGA X hole are similar although enlargement of the region at the edge of the hole reveals an oscillation of the GGA X hole. The SIE mimics now short-range rather than long-range correlation effects, which are typical of an atom with an increased number of electrons (the larger the number of atoms and the more contracted the atomic orbitals are the larger are the dynamic correlation effects).

The X-holes for the the β electron being located at P2 will not change very much if the the broken-symmetry solution is applied (Fig. 5c). Again, the β exchange hole is localized at P2, which will be also true if the reference electron is at P1. The latter situation is however less interesting because it does have little influence on the SIE energy as discussed above. For the ionic solution the SIE mimics just short range correlation effects reflecting the peculiar form of the intraelectronic UGGA exchange hole (dotted curve with stars in Fig. 5c), which is reminiscent of the spherically symmetric form of the

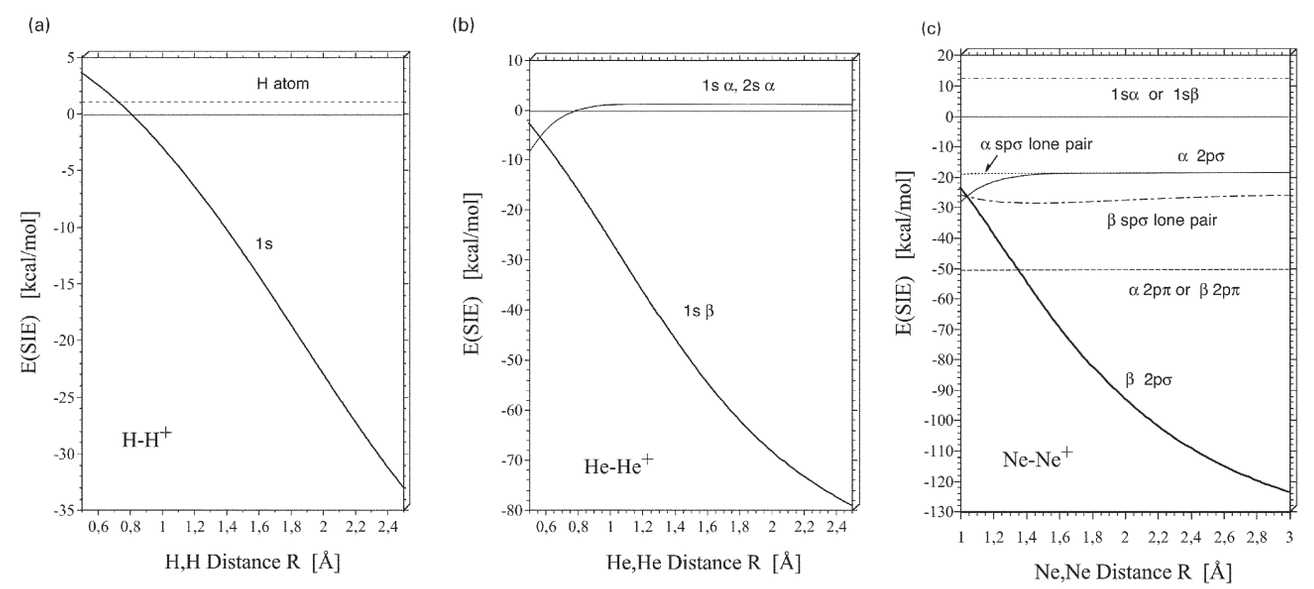

Fig. 3 Orbital contributions to the self-interaction error for (a) H_2^+, (b) He_2^+, and (c) Ne_2^+ both for the ionic and the covalent solutions. All calculations are done with Dunning's cc-pVTZ basis set.[50]

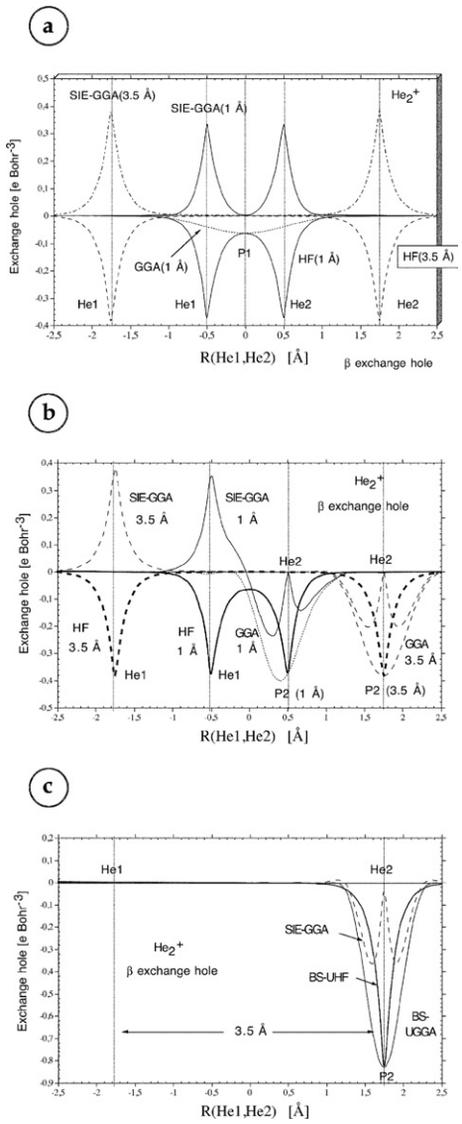

Fig. 4 Graphical representation of the exchange hole for the β electron of He_2^+ ($^2\Sigma_u$) calculated along the bond axis at the HF and GGA(PW91PW91) levels of theory using the symmetry-adapted solution for separation distances R of 1 and 3.5 Å. (a) The reference electron is positioned at the midpoint of distance R(He1,He2). (b) The reference point is at nucleus He2 (position P2). (c) The X holes for the broken-symmetry solutions at a distance R of 3.5 Å are shown for the position P2 of the β electron. Note that for the one-electron case, the HF exchange hole is equal to the SIC-DFT exchange hole. The SIE part of the DFT exchange hole is given as the difference between DFT and SIC-DFT exchange hole. All calculations are with a cc-pVTZ basis set.[50]

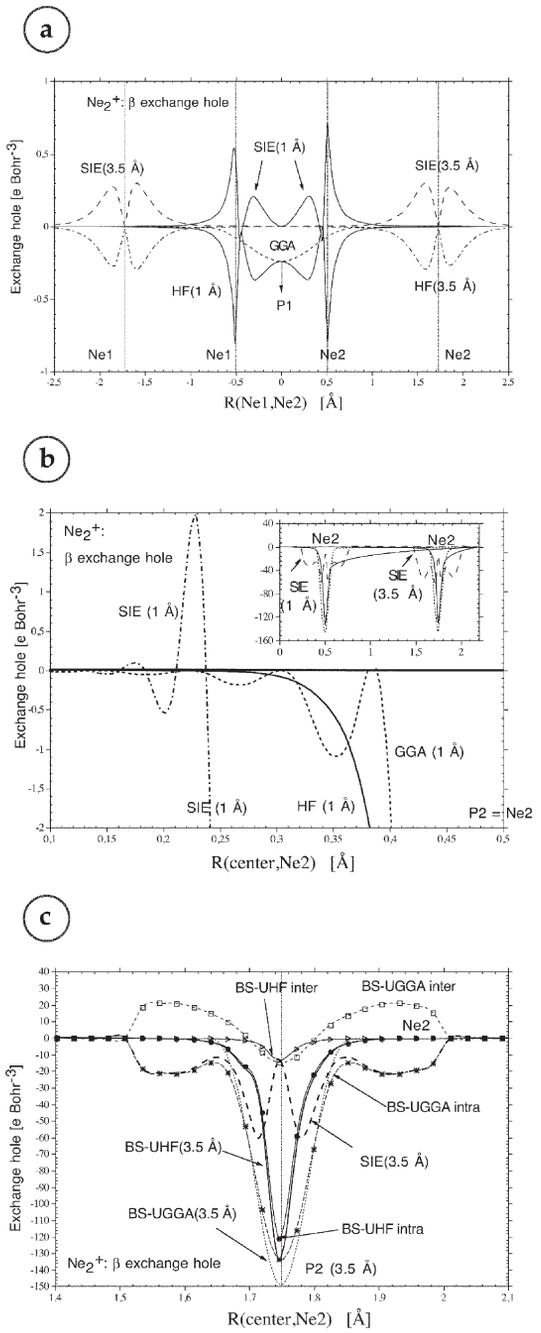

Fig. 5 Graphical representation of the exchange hole for the highest β electron of Ne_2^+ ($^2\Sigma_u$) calculated along the bond axis at the HF and GGA(PW91PW91) level of theory for separation distances of 1 and 3.5 Å. (a) The reference electron is positioned at the midpoint of distance R(Ne1, Ne2). (b) The insert gives the X holes for the reference electron at the bond center and $R = 1$ and 3.5 Å. The left part of the hole for $R = 1$ Å is enlarged in the figure. (c) The X holes for the broken-symmetry solutions at a distance R of 3.5 Å are shown for the position P2 of the β electron. Intra- and interelectronic exchange holes are also shown. All calculations are with a cc-pVTZ basis set.[50]

2s orbital with its nodal surface. The interelectronic GGA exchange hole (which has no relevance for the SIE) cancels largely the intraelectronic part in the edge regions of the total hole where a slightly unbalanced cancellation is responsible for the oscillations of the total GGA hole. Fig. 5c reveals also that the interelectronic hole of exact exchange is very small (solid line with triangles in Fig. 5c) whereas interelectronic exchange is substantial in the edge regions of the hole to cancel the deviation of intraelectronic GGA exchange from exact exchange.

Several important conclusions result from the exchange hole representations in Figs. 4 and 5: (1) The SIE mimics a non-dynamic correlation effect for the β electron in radical cations **2**–**6**, which increases with increasing distance R. (2) For **2**, there cannot be any other than non-dynamic correlation effects. However, with increasing number of electrons in the series **2**, **3**, **4**, **5**, **6**, the SIE accounts for an increasing amount of short range (dynamic) correlation effects for increasing R, which in the case of **6** dominate the non-dynamic effect since the latter are still just for one fictitious partner of the β electron. This means that in eqn. (3) the value of J_A increases whereas the Coulomb repulsion term still refers to two halves of an electron repelling each other. (3) The correction of the SIE converts the intraelectronic GGA hole into the intraelectronic HF hole. This however leads to an error caused by the relatively large interelectronic GGA exchange. This is true for both covalent and ionic solutions as long as the reference electron is at the core or in the valence region. It does not play

any role for the reference electron being at the bond middle point.

In the following we have to consider whether the symmetry-adapted or the broken-symmetry solution leads to a better description of the dissociating radical cations with three-electron bonds.

3.3 Covalent and ionic state of the dissociating molecule

The dissociation of a symmetric molecular cation will always lead to a neutral and an ionic fragment, *i.e.*, the positive surplus charge gets localized at one of the fragments and the symmetry of the original molecule is broken. However, a quantum-chemical description may predict a decay into either an ion and a neutral fragment (ionic state) or two identical fragments carrying a charge of $+1/2$ each (covalent state), depending on which state is lower in energy for the supermolecule in the limit of large interaction distances R.

Table 5 lists the energies of the covalent and ionic state at an interaction distance of 10 Å for a variety of DFT and wave-function methods. In addition, the lowest eigenvalues of the electronic Hessian for the two states, which is a measure for their electronic stability,[58,59] are shown where available. For polyatomic radical cations, the energy ordering of covalent and ionic state is influenced by geometry distortions within the fragments, which always favor the ionic rather than the covalent state. Therefore, we restrict this investigation to the diatomic molecules **2** and **6** because geometry effects do not play any role for these radical cations.

For both molecules, standard BLYP favors the covalent state by about 90 kcal mol^{-1}. The covalent state is stable ($\lambda(\mathbf{2}) = 0.545$; $\lambda(\mathbf{6}) = 0.530$; Table 5) whereas the ionic one is unstable ($\lambda(\mathbf{2}) = -0.190$; $\lambda(\mathbf{6}) = -0.581$) and difficult to locate. With increasing a_{HF} the ionic state become less unstable (Table 5). For HFLYP, the ionic state is lower in energy and stable whereas the covalent one becomes unstable. At the HF level, the ionic state is already 14.6 and 35 kcal mol^{-1} lower in energy than the covalent state of the two molecules **2** and **6** (Table 5). A comparison of HFLYP and HF reveals that the inclusion of the LYP correlation functional stabilizes the covalent state by 6.8 kcal mol^{-1} (**2**) or 2.7 kcal mol^{-1} (**6**), respectively, whereas it makes the ionic state less stable (reduction of $\lambda(\mathbf{2})$ from 0.096 to 0.011 and $\lambda(\mathbf{6})$ from 0.225 to 0.205) and the covalent one less unstable (increase of $\lambda(\mathbf{2})$ from -0.085 to -0.066 and $\lambda(\mathbf{6})$ from -0.205 to -0.191; Table 5).

Table 5 Energies and electronic stability for the covalent and ionic ground states of **2** and **6** at different levels of theory[a]

Molecule	Method	E_{cov}	$E_{ion} - E_{cov}$	λ_{cov}	λ_{ion}
2	BLYP	−5.04761	92.17	0.545	−0.190
	B3LYP	−5.02800	72.49	0.434	−0.160
	BH&HLYP	−4.96852	41.90	0.245	−0.032
	HFLYP	−4.89224	−7.30	−0.066	0.011
	HF	−4.83688	−14.56	−0.085	0.096
	SCSIC-BLYP	−4.88097	−7.33		
	MP2	−4.88660	−4.15		
	CISD	−4.89887	−0.18		
	CCSD	−4.89882	−0.21		
	CCSD(T)	−4.89910	−0.03		
6	BLYP	−257.25876	91.95	0.530[b]	−0.581
	B3LYP	−257.23580	66.83	0.389[b]	−0.425
	BH&HLYP	−257.12858	28.80	0.169[b]	−0.184
	HFLYP	−257.06194	−32.30	−0.191	0.205[b]
	HF	−256.34074	−35.00	−0.205	0.225[b]
	SCSIC-BLYP	−256.61324	−11.31		
	MP2	−256.83884	7.19		
	CISD	−256.80554	−7.80		
	CCSD	−256.83572	−2.85		
	CCSD(T)	−256.84670	−0.29		

[a] Absolute energies in E_h, relative energies in kcal mol^{-1}. Parameter λ denotes the lowest eigenvalue of the stability matrix. [b] There are eigenvalues equal to zero that are related to excitations within the quasidegenerate 2p orbitals. The table shows the first positive eigenvalue.

Correlated wave-function methods lead to smaller energy differences between ionic and covalent states ($|E(\text{ion}) - E(\text{cov})| < 8$ kcal mol^{-1}; Table 5) than standard DFT. Whereas MP2 stabilizes the ionic state for **2** and the covalent one for **6** all other methods favor the ionic state for both molecules. CCSD(T) provides within 0.3 kcal mol^{-1} the same energy for both states.

Given that the dissociation of radical cations proceeds asymmetrically, it appears plausible that a correct quantum-chemical description of the dissociation should predict the ionic state of the supermolecule lower in energy than the covalent one. However, the dissociation is a dynamic process where the system is not in its electronic ground state. The electronic ground state for any interaction distance R is covalent for reasons of symmetry. For increasing R, the excitation energy between the covalent ground state and the corresponding antibonding state decays exponentially. This means that bonding and antibonding states become quasi-degenerate, and one can superimpose the two eigenstates to two equivalent ionic states (and a continuum of partially ionic states), all of which have nearly the same energy. These ionic states are quasistationary rather than stationary, with a lifetime growing exponentially with R. The asymmetric dissociation can be described in terms of these quasistationary states. The electron jumps back and forth between the two quasistationary ionic states. As R increases, the probability that the electron tunnels from one fragment to the other decreases rapidly, and finally the electron remains at one of the fragments. A correct quantum-mechanical description should thus predict a covalent ground state that is nearly degenerate with its antibonding counterpart. The stability of this state with respect to a transition into the ionic state has to be positive and to decay exponentially with R. The ionic and partially ionic states are not electronic eigenstates for any finite R. They can, however, be made stationary, and thus feasible for a quantum-mechanical calculation by applying a weak homogeneous electric field along the bond axis. This is equivalent to constraining the dipole moment of the molecule relative to its bond center.

Thus, neither DFT nor HF provide a correct description of the balance between electronic and ionic state of symmetric radical cations: Whereas HF predicts the ionic state as electronically stable and lowest in energy, standard DFT yields a covalent ground state with a non-vanishing positive stability and a pair of equivalent ionic states whose energy does not converge to that of the covalent state for $R \to \infty$. Correlated wave-function methods, which are based on a HF reference, partly correct the inconsistency in the HF description and correct the ionic HF state towards the correct covalent one. CCSD(T) predicts differences $E(\text{ion}) - E(\text{cov})$ of just -0.03 (**2**) and -0.29 kcal mol^{-1} (**6**, Table 5) and, by this, represents clearly the most accurate method used in this work.

According to calculated energy differences $E(\text{ion}) - E(\text{cov})$, SC-SIC-BLYP seems to offer a significant improvement relative to DFT. The ionic state is predicted by 7.3 or 11.3 kcal mol^{-1}, respectively, (Table 5) lower in energy than the covalent one. We will show in Subsections 3.4 and 3.5 that these energy differences are actually due to a fortuitous cancellation of errors, from which SIC-DFT still suffers.

3.4 Non-dynamic correlation effects influencing the dissociation of three-electron bonds

The non-dynamic correlation effects for the dissociating three-electron bond are best contrasted against those non-dynamic

effects experienced during the dissociation of an electron-pair (even-electron) bond, for example in the simple case of the H_2 molecule (**10**).

Fig. 6a shows the dissociation curve for **10** calculated at different levels of theory. As is well known, spin-restricted DFT fails to describe the dissociation limit properly but predicts a positive limit for the relative energy, *i.e.*, the stretched molecule has a higher energy than the fragments. For RBLYP the limit of $|D_e|$ is about 44.6 kcal mol^{-1} and is approximately reached for $R \approx 5$ Å. For HFLYP, the limiting value of the relative energy is as high as 163.6 kcal mol^{-1}. Besides, HFLYP pretends that there is a Coulomb attraction between the two fragments with the product of the charges being 1/2 unit charge, such that D_e converges slowly towards its limiting value. If spin-symmetry breaking is allowed both BLYP and HFLYP will provide the correct dissociation limit. BS-UBLYP agrees with the CISD reference within 2 kcal mol^{-1} *i.e.* less than the resolution in Fig. 6a, whereas BS-UHFLYP predicts too high relative energies in the region around the R → U bifurcation. The use of SIC-DFT does not improve the accuracy. The P-SIC-RBLYP dissociation curve shows the same behavior as the RHFLYP curve, with a limit for the relative energy of 169 kcal mol^{-1}. BS-P-SIC-UBLYP behaves very similarly as BS-UHFLYP. The SCSIC-BLYP level of theory is for **1** equivalent to the HFLYP level.

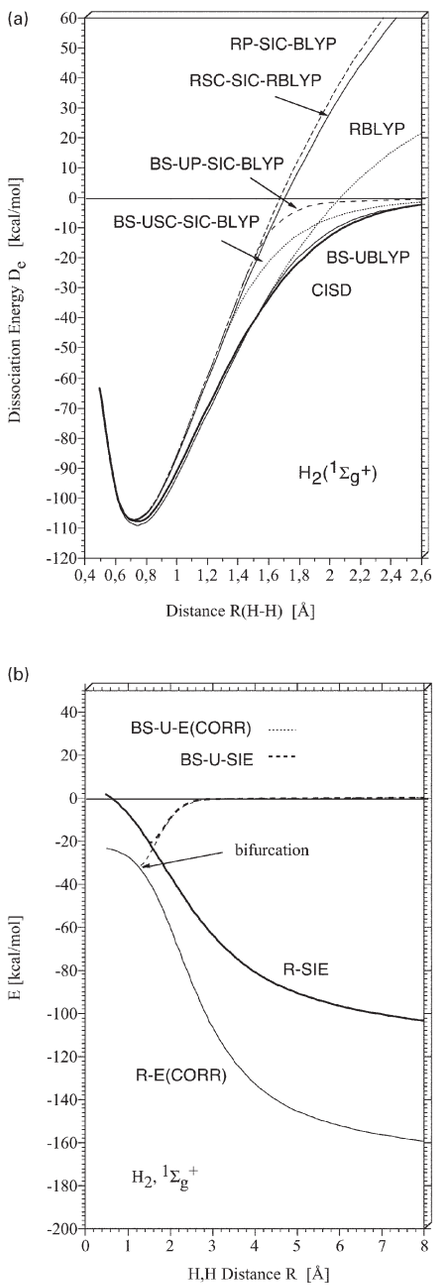

Fig. 6 (a) Dissociation curves for H_2 calculated with the DFT and wave-function methods described in Subsection 3.2. (b) Self-interaction error (SIE) for H_2 calculated at the spin-restricted (R) and spin-unrestricted (U) BLYP[45,46] level, and correlation energy E_{corr} for the spin-restricted and spin-unrestricted treatment of H_2. Dunning's cc-pVTZ basis set[50] was used for all calculations. Experimental values from K. P. Huber and G. Herzberg, *Constants of Diatomic Molecules*, Van Nostrand Reinhold, New York, 1979.

The dissociation of an even-electron bond causes strong left-right correlation effects between the two bond electrons. In terms of configurations, this means that the excited $1(\sigma_u)^2$ configuration becomes occupied with a weight that for $R \to \infty$ becomes equal to that of the ground-state $(1\sigma_g)^2$ configuration (see Fig. 7a). These left–right correlation effects, which may contribute 100 kcal mol^{-1} and more to the total energy, reduce the charge fluctuations at the fragments, suppressing zwitterionic contributions and, accordingly, unreasonable Coulomb attraction effects between the fragments. Coverage of left–right correlation and consequently suppression of zwitterionic configurations, is thus crucial for an appropriate description of the dissociation of electron pair (even electron) bonds. Standard DFT correlation functionals provide no description for non-dynamic correlation effects because they are designed for an accurate description of dynamic correlation. This shortcoming can be seen most clearly for RHFLYP, which behaves qualitatively as RHF in spite of the correlation term. RBLYP provides no explicit description of the non-dynamic correlation effects either. However, as has been discussed above (see also refs. 6, 7 and 13), the SIE mimics an increasing amount of left–right correlation effects as R increases. Consequently, the SIE in BLYP suppresses the charge fluctuations, and the RBLYP dissociation energy becomes constant for R above 5 Å. However, RBLYP is not able to account for all non-dynamic correlation effects.

In Fig. 6b the SIE and the correlation energy for **10** are shown both for the spin-restricted and the spin-unrestricted case as a function of R to illustrate the relationship between the SIE and the correlation energy. The correlation energy was calculated as the difference between HF and CISD energies; the difference between the correlation energy obtained by wave-function theory and that obtained by DFT can be ignored here. For the spin-restricted case, the SIE accounts for an increasing part of the correlation energy. In addition, the SIE cancels the artificial Coulomb attraction between the fragments. For the spin-unrestricted description, both the correlation energy and the SIE possess a negative peak at the bifurcation point. This confirms the statement in the previous

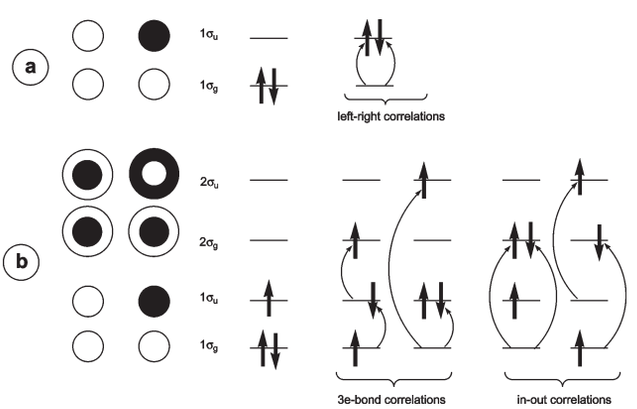

Fig. 7 Schematic representations of those configurations of **2** that lead to (a) the left–right correlations in the case of the electron pair bond of the three-electron bond correlations and the in–out correlations.

subsection that the UHF/UDFT description of bond breaking is least accurate around the bifurcation point, where the non-dynamic correlation effects are relatively strong but are not simulated by the symmetry breaking. However, the SIE partly compensates this shortcoming (Fig. 6b). Owing to the SIE, standard BS-UDFT provides a more balanced description of bond breaking, including the region around the bifurcation point, than HF or HF-KS schemes do.

In a three-electron bond, left–right correlation effects analogous to those found in two-electron bonds cannot be established. In the case of **2**, the α LMOs at both atoms are occupied, and the α electrons can thus not avoid the β electron by jumping back and forth between the He atoms. There is, however, another type of long-range correlation effect[39] that is specific to three-electron bonds and, therefore, will be called "3e-bond correlation" in the following. When an electron is added to a fragment, it will influence the electronic structure of this fragment in two ways: First, it will establish dynamic correlation effects (in–out, angular) with the other electrons. Second, the density distribution of the other electrons will become more diffuse, which reduces Coulomb repulsion between the extra electron and the other ones. If the extra electron is localized at the fragment this can be regarded as an orbital relaxation.

If, however, the extra electron is delocalized over two fragments, this will lead to the fact that the shape of the orbitals depends on the location of the extra electron. Hence, in addition to the short-range dynamic correlation effects, there is long-range correlation between the bonding β electron and the other electrons. It is reasonable to classify this correlation effect as non-dynamic for two reasons: Firstly, the effect acts over the whole separation distance *R*, *i.e.*, it is long-ranged. Secondly, the response of the remaining electrons depends not on the exact position of the bonding electron but only on the fragment at which it resides. In Fig. 7(b), the leading excited configurations related to 3e-bond correlation are shown for **2**. Both of them include an $1\sigma_g \rightarrow 1\sigma_u$ excitation of the β electron, which is coupled with an excitation of one of the α electrons either $1\sigma_u \rightarrow 2\sigma_g$ or $1\sigma_g \rightarrow 2\sigma_u$.

In all excitations, the electrons change between orbitals of different symmetry, which reflects the relationship of these excitations to the left–right movement of a bonding electron. Note, however, that the excitations of the α electron in first order do not affect its probability to be found at one or the other fragment. This distinguishes the 3e-bond correlation effects from the left–right effects in 2e-bonds. The 3e-bond correlation effects have to be distinguished not only from left–right correlation effects but also from in–out correlation. In Fig. 7(b), the leading configurations for the description of in–out correlation are shown. These configurations do not include excitations from bonding to antibonding orbitals and *vice versa* in line with the fact that these correlation effects are not related to the left–right movement of the electrons. The 3e bond correlation makes a considerably smaller energy contribution, typically around 10 kcal mol^{-1}, than left–right correlation effects.

At large *R*, the 3e-bond correlation energy converges to a constant value, which is the same for the bonding and the antibonding state. This means that for $R \rightarrow \infty$, the 3e-bond correlation effects in the covalent state make the same contribution to the energy as the corresponding orbital relaxations in the ionic state. This in turn implies that methods that cannot describe the 3e-bond correlation effects will have a tendency to overstabilize the ionic state relative to the covalent one. This explains why HF always predicts an ionic ground state for 3e-bonded systems (see the results for **6** as an example) and HFLYP often predicts ionic ground states, especially for large *R*. Correlated wave-function methods based on the HF reference may predict either an ionic or a covalent ground state for 3e-bonded systems: Methods that tend to exaggerate non-dynamic correlation effects such as MP2[62] will tend to predict a covalent ground state while variational methods such as CISD should predict an ionic ground state. High-level *ab-initio* methods such as CCSD(T) annihilate to a large extent the inconsistencies between the HF references for the two states as is documented for **2** and **6** in Table 5.

Standard DFT, similarly as HF, cannot describe the 3e-bond correlation effects properly because the DFT correlation functionals are not suitable to describe this specific form of long-range correlation effects. The question arises whether the SIE can mimic these correlation effects in a similar way as left–right correlation for the even-electron bonds. This is not the case for two reasons: (a) The SIE energy contribution is much larger than the typical 3e-bond correlation energy. This explains that standard DFT predicts covalent ground states for 3e-bonded systems even though the 3e-bond correlation effects in the covalent state are not covered. (b) The SIE behaves differently than the 3e-bond correlation energy as $R \rightarrow \infty$. For the dissociation of 3e-bonds, similarly as in the case of 1e-bonds, the SIE does not improve the DFT description but leads even to a qualitatively incorrect description.

Long-range correlation effects similar to the 3e-bond correlations occur between the bonding electron and all other electrons in the system. This means in particular that an analogous type of correlation effects occurs in 1e-bonded systems between the bonding α electron and all other electrons. However, not all of these correlation effects make a relevant contribution to the total energy. Only orbitals that are energetically close to, and equally diffuse as, the bond orbital will give non-negligible contributions to the correlation energy. As a consequence, 1e-bond correlation effects may be negligible, whereas 3e-bond correlation effects between the bonding β electron and the two α electrons in the bond are always relevant for the total energy.

3.5 Interelectronic exchange effects influencing the dissociation of three-electron bonds

DFT exchange functionals are approximate not only with respect to the electron self-interactions but also with regard to interelectronic exchange. This is reflected by the interelectronic exchange holes shown for **6** in Fig. 5. For HF, interelectronic exchange will correspond to a long range effect if the reference electron is bonding and in the bond region. Standard DFT fails to describe this effect. If the reference electron is at the nucleus (Fig. 5c), interelectronic HF exchange is small (there is little chance of finding a second electron of the same spin there) whereas interelectronic DFT exchange is considerable. As long as the standard X functional is used the effect of interelectronic exchange is compensated by intraelectronic exchange (Fig. 5c). This changes for SIC-DFT, for which interelectronic exchange is no longer compensated and therefore becomes a serious error.

A simple estimate similar to that for eqn. (3) and presented in the Appendix reveals that the error in the interelectronic DFT exchange of radical cations with a three-electron bond leads to an artificial stabilization of the covalent state relative to that of the ionic state that (i) is smaller than the SIE and (ii) converges quickly as *R* increases. Nevertheless, the error in the interelectronic exchange acts together with the SIE and leads to the large overestimation of the stability of dissociating radical cations. It has also serious consequences for the dissociation limit of the radical cations with three-electron bonds.

The DFT error in the description of the interelectronic exchange can partly compensate the overstabilization of the ionic state predicted by the BS-UHF description. SIC-DFT, for which the SIE is corrected but the DFT error in the interelectronic exchange is left, provides a description of ionic and covalent states that seems to be more balanced than both

standard DFT and HF descriptions. One should, however, be aware that this cancellation will be accidental and that there are no principal reasons why 3e-bond correlation energy (provided by BS-UDFT) and the error in the interelectronic exchange should be always comparable in size so that they largely cancel.

3.6 The SIE of the fragments

The dissociation energy of radical cations is influenced by the SIE of both the dissociating molecule and the fragments. In general, the orbitals in the fragments are localized, and the resulting SIE is relatively small and compensates partly the SIE for the core electrons in the supermolecule. There is, however, a subtle point in the SIC-DFT description of $\mathbf{7}^{+\bullet}$ related to the fact that the Perdew–Zunger SIC-DFT procedure is not invariant with respect to rotations among the occupied orbitals: $\mathbf{7}^{+\bullet}$ is known to be planar, which is confirmed both by wave-function and standard DFT calculations. SIC-DFT, in contrast, predicts a pyramidal ground state. The P-SIC-BLYP geometry has a pyramidalization angle of 25° (Scheme 1) and an energy 5.20 kcal mol^{-1} below that of the planar form. SC-SIC-BLYP at the P-SIC-BLYP geometries gives an energy lowering of 6.40 kcal mol^{-1} due to pyramidalization.

This result can be traced back to the different orbital localization patterns in the planar and the pyramidal states of $\mathbf{7}^{+\bullet}$: For the planar state, the localization of the α valence orbitals gives three N–H bond orbitals with sp^2 character at the N atom and a π(N) orbital. The N–H bond orbitals have an SIE of −3.3 kcal mol^{-1} each whereas the SIE of the π orbital amounts to −30.7 kcal mol^{-1}. If the molecule is pyramidized the π orbital and the N–H bond orbitals are mixed. The π orbital gets partial s character and at a pyramidalization angle of 25° its SIE decreases to −13.6 kcal mol^{-1}. The N–H bond orbitals in turn get increased p character, which increases their SIE to −6 kcal mol^{-1} per orbital. The SIE of the β valence electrons changes by less than 0.2 kcal mol^{-1} per orbital. Altogether, the SIE of the α valence orbitals is decreased from −40.7 kcal mol^{-1} to −31.7 kcal mol^{-1} by pyramidalization, *i.e.* by 9.0 kcal mol^{-1}. Changes in the SIE of the remaining orbitals and changes in the nuclear attraction and relaxation effects lead finally to the stabilization energy of 6.40 kcal mol^{-1} for the pyramidal form.

The SC-SIC-DFT dissociation curves for **3** shown in Fig. 3a and the D_e value in Table 4 are calculated based on the (planar) CCSD(T) geometry for $\mathbf{7}^{+\bullet}$. Consequently, the dissociation energy of the molecule becomes too large by 5.20 kcal mol^{-1} for P-SIC-BLYP and 6.40 kcal mol^{-1} for SC-SIC-BLYP, which means that the correct P-SICDFT D_e value of **3** is 33.80 rather than 39.00 kcal mol^{-1}. The same holds for the P-SIC-BLYP dissociation energy, which is actually 32.79 rather than 39.19 kcal mol^{-1}. Clearly, the lack of unitary invariance in SIC-DFT leads to a serious deterioration of the accuracy.

4. Outlook: Requirements for a SIE-free exchange-correlation functional

A number of important conclusions can be drawn from the investigation of the radical cations with three-electron bonds.

(1) In general, a correct description of a dissociating three-electron bond should predict a bonding covalent ground state for all interaction distances R. For large R, this state is nearly degenerate with its antibonding counterpart. Superposition of bonding and antibonding states leads to a continuum of quasidegenerate states that are partly or fully ionic. These states are quasistationary for any finite R but can be made stationary, *e.g.*, by applying a weak homogeneous electric field along the bond axis. A correct quantum-chemical description of the dissociation must thus predict a covalent ground state for all R where the stability with respect to a translation of the valence electron to one of the fragments must decrease exponentially with increasing R. If a calculation method favors either the covalent or the ionic state, this will indicate an inconsistency. The energy difference between the two states is a direct measure for this inconsistency.

(2) For polyatomic cations, the ionic state mostly becomes the ground state by virtue of geometry relaxations. This effect is small, although present, for **4** and **5**. For **3**, in contrast, the neutral fragment becomes pyramidal by a second-order Jahn–Teller distortion whereas the ionic fragment remains planar, which leads to considerable stabilization of the ionic state. It should, however, be emphasized that the statements in (1) remain valid as long as ionic and covalent state are compared at the same geometry.

(3) Standard KS-DFT gives an incorrect description of the dissociation of three-electron-bonds: (i) For large R, the supermolecule is substantially lower in energy than the dissociated fragments, in some cases even lower than the radical cation itself (see **2** and **6**). (ii) The dissociation curve passes for increasing R through a transition state, beyond which the fragments appear to repel each other. Also, the description of covalent and ionic state is inconsistent: The covalent state is lower in energy than the ionic one and has a non-vanishing positive stability even for large R.

(4) The inconsistencies in the DFT description of three-electron-bonds can be traced back to the SIE of the bonding (delocalized) β electron. As R increases, the SIE of the bonding electron takes the form $1/(4R)+ZJ_A$, where Z is a negative constant depending on the approximate X functional used and J_A is the self-repulsion energy of the β electron. The $1/(4R)$ term is related to the artificial Coulomb repulsion mentioned in (3), whereas ZJ_A accounts for the incorrect dissociation limit. The contribution from the bonding β electron dominates the total SIE. The two α electrons of the three-electron bond are localized at one of the fragments each. Consequently, their contribution to the total SIE is small and independent of R, except for small R. As the dissociations are considered, the SIE of the α electrons is in most cases partly compensated by the corresponding SIE of the isolated fragments.

(5)(a) The function SIE(R) possesses an inflection point because for R around r_e the SIE becomes a concave function of R. This is due to the fact that in the equilibrium region (i) the spatial extent of the bond orbital is no longer just dominated by R and (ii) the X–H bond orbitals extend because of hyperconjugation or steric repulsion effects. Any extension of the localized X–H bond orbitals makes the SIE more negative for decreasing $R<r_e$.

(5)(b) For small R, two situations can be distinguished. (I) The hyperconjugative effects are small (just second order hyperconjugation as in **3** or **4** plays a role) and at the equilibrium the SIE given by the convex function $1/(4R)+ZJ_A$ dominates. Standard DFT overestimates bond lengths and underestimates the frequencies of the X–X stretching vibrations as was found for all radical cations investigated. (II) Hyperconjugation is strong (first order hyperconjugation plays a role) and at the equilibrium the concave behavior of the SIE plays the dominant role. Standard DFT yields too short a bond length and exaggerated X–X stretching frequencies. This situation is found for the radical cation H_2BBH_2 that possesses a one-electron bond.[11]

(6)(a) Investigation of the DFT β exchange hole (partitioned in SIC-DFT and SIE part) reveals that the SIE mimics non-dynamic correlations between the bonding β electron and a second electron that is not present in reality. These non-dynamic correlation effects lead to an artificial stabilization that increases with increasing R. The same effects are also present in the DFT description of the dissociation of electron-pair

(even-electron) bonds: There, the SIE mimics part of the non-dynamic correlation between the two paired bonding electrons, which is missing in a RHF description. Consequently, RDFT, though not correct, reduces the inconsistencies of RHF in the dissociation limit.

(6)(b) With an increasing number of core electrons in the series **2** to **6**, the value of J_A increases. The nature of the SIE changes is clearly reflected by the exchange holes: Although the non-dynamic correlation effects associated with the bonding β electron remain, the SIE mimics a large amount of short-range (dynamic) electron correlation. The dynamic correlation effects increase with increasing R until they reach their maximum value defined by the artificial self-exchange $Z\,J_A$. Hence, standard DFT exaggerates the stability of the dissociating radical cations by mimicking long-range effects for the bonding β electron and short-range dynamic electron correlation of the β with all other electrons.

(6)(c) BS-UHF and BS-UDFT improve the wavefunction of the dissociating neutral molecules by implicit two-configurational descriptions. The BS-UHF and the BS-UDFT exchange holes of the bonding β-electron are both localized. They differ only in some short-range correlation effects simulated by the SIE. BS-UDFT leads to a balanced description of the whole dissociation of the radical cation with a three-electron bond, including the recoupling region, neutral molecules by implicit two-configurational descriptions.

(7) SIC-DFT allows correction of the inconsistencies in standard DFT calculations. However, the SIE has to be corrected self-consistently for this purpose. A P-SIC calculation overcompensates the error of the standard-DFT description considerably leading to an energy for the supermolecule well above that of the fragments.

(8) An additional stabilization of the covalent state in a DFT description is caused by the error in the interelectronic exchange hole, which is often delocalized for exact exchange, however always localized for approximate DFT exchange. In the case of the dissociating radical cation, the error due to a simplification of interelectronic exchange is constant for large R. SIC-DFT does correct the SIE, however, the error in the interelectronic exchange remains.

(9)(a) In three-electron-bonds, the two α electrons avoid the β electron to minimize Coulomb repulsion. In the ionic state, this leads to an orbital relaxation that makes the orbitals at the ionic fragment more diffuse than at the neutral one. In the covalent state, this mutual avoidance of the three bond electrons results in a specific form of non-dynamic correlation effects, called *3e-bond correlation effects* here, that are different both from the left–right correlation effects in even-electron bonds and the (dynamic) in–out and angular correlation effects. A balanced description of ionic and covalent state requires that these correlations are covered. The energy gain due to these correlation effects is R-independent as long as the fragments are well-separated.

(9)(b) UHF can describe the orbital relaxations in the ionic state but not the 3e-bond correlations in the covalent one. Hence UHF predicts a stable ionic ground state for large R. This is not, as claimed in the literature,[33,38] an advantage of UHF but an indication of its inconsistency. Correlated wave function methods may predict either a covalent or an ionic ground state, depending on the method used. CCSD(T) provides the best description in so far as the energy difference between ionic and covalent state is negligible.

(9)(c) DFT, similarly as UHF, does not cover the 3e-bond correlation effects. Of course, the SIE compensates this shortcoming although not in a specific way: The SIE is (i) considerably larger than the 3e-bond correlation energy and (b) contrary to the 3e-bond correlation effects strongly R-dependent.

(10)(a) SIC-DFT leads to a decreased energy difference between ionic and covalent dissociation. This, however, is not an indication for an improved performance of SIC-DFT, but simply the result of a large error compensation: The overstabilization of the ionic state in a BS-SIC-DFT description is counteracted by the error in the interelectronic DFT exchange favoring the covalent state. However, there is no exact compensation between the two opposing effects, and the ionic state for **2** and **6** is still 7 kcal $mol^{-1}$and 11 kcal mol^{-1}, respectively, below the covalent one.

(10)(b) The RSIC-DFT description of the radical cations suffers from two important shortcomings: a lack of long-range 3e-bond correlation effects and the oversimplified interelectronic exchange, which leads also to long-range effects. There is however a third deficiency of SIC-DFT, which has so far been overlooked in the literature.

(10)(c) The lack of unitary invariance for the SIC-DFT energy can lead to unphysical symmetry-breaking effects in the SIC-DFT description of the fragments. An unrealistic pyramidalization of $\mathbf{7}^{+\bullet}$ lowers its SC-SIC-BLYP energy by 6.40 kcal mol^{-1}, whereas the correct ground state is planar. Consequently, care is required to select the appropriate reference for the relative energy in the dissociation of radical cations. We note that a similar effect is found for the dissociation of the ethane radical cation.[11]

The problems discussed in connection with a DFT description of radical cations with one- or three-electron bonds are also of relevance for DFT descriptions in general. DFT transition states of radical reactions with closed shell systems are predicted too low in energy, which is a result of the SIE. The transition states of XH_n (X = F, O, N, C and n = 0, 1, 2, 3) with H_2 are typical examples for this.[63] The simplest of these reactions, namely the reaction $H + H_2$ was preliminarily investigated with P-SIC-DFT.[16,21,64] The SIE leads in this case of an underestimation of the barrier by 10 kcal mol^{-1}. Furthermore the reactions of ozone with various organic substrates imply transition states with an odd number of electrons, which are typically underestimated by standard DFT.[65,66] The DFT barriers of H abstraction reactions are always too low.[67] DFT descriptions of the reactions of singlet biradicals can be flawed by the same error. In general, any reaction, in which the chemical processes of bond breaking and forming no longer involve an even number of electrons, is sensitive to the SIE.

Odd-electron situations are also experienced in charge-transfer complexes.[32] The description of donor–acceptor complexes can lead to substantial SIEs, especially if the acceptor is a dication. The calculation of transition metal complexes by DFT becomes particularly problematic because of the SIE. There are several studies of iron complexes in the literature where the SIE leads to unbalanced reaction and activation energies.[68]

The SIE often leads to the vanishing of transition states and generates artificial minima (see $\mathbf{7}^{+\bullet}$ above). In the reaction of atomic oxygen with dimethylether, Sander and co-workers observed this problem.[69] Artificial minima have also been found in hydroxyl and hydroperoxyl radical reactions.[65,66]

Singlet–triplet splittings can also be flawed by the SIE: the singlet is normally described by RDFT, which leads to a normal stabilizing SIE. For the triplet, the SIE is normally small so that the singlet–triplet splitting depends on the question whether the singlet is stabilized in the right way. For many closed shell systems and biradicals[70] this is indeed the case. Properties that depend on the correct calculation of singlet–triplet splittings are reasonably described. The NMR spin–spin coupling constants[71] are an example of this case because the Fermi contact term requires reliable singlet–triplet excitations. If they are underestimated (overestimated), the calculated Fermi contact term is too large (small), which can only be corrected by using less (more) exact exchange.[71] There are additional SIE effects which can have an influence on the singlet–triplet splittings: For a BS-UDFT description there is no orthogonality constraint between the two singly occupied

orbitals and therefore, relatively compact orbitals result. In the triplet, the singly occupied orbitals are orthogonal, which may lead to delocalized orbitals due to their mutual steric repulsion. Accordingly, the SIE becomes more negative, which may act as a second order effect leading to slightly decreased singlet–triplet splittings.

Despite the fact that the SIE has been extensively discussed in the literature,[3–42] there are still DFT investigations in which the problem is totally ignored and questionable DFT results are presented at length in the literature. It seems that especially in transition metal investigations the problem is not recognized. Baerends and co-workers[23] have set up rules how to identify an odd electron situation, however for charge transfer reactions it is always best to test the calculated charges and draw from there appropriate conclusions with regard to the importance of the SIE. It is also necessary to consider in this connection the XC functional used. The SIE of the X and the C functional can cancel each other partially as in the case for PW91PW91.[5–7] Since the LYP functional does not possess a SIE, BLYP does not benefit from cancellation and the SIE is relatively large.[5–7]

Considering that the SIE of approximate XC functionals concerns not only the radical cations but also many other electronic systems it is clear that there have been many attempts to develop SIE-free XC functionals. The SIC-DFT methods based on the Perdew–Zunger approach are too costly to represent a solution to the problem. However, even without this technical disadvantage, SIC-DFT causes more problems than it solves:

(a) As shown for **10** (Fig. 6a), BS-USIC-DFT provides a poor description of the recoupling region (1.3–1.9 Å) of the dissociation of the electron-pair bond. The description can be improved by orbital relaxation provided by SC-SIC-DFT, however even then deviations from the correct description (CISD dissociation curve, Fig. 6a) are large. SIC-DFT incorrectly recognizes an odd-electron situation in the recoupling region (there are now two separated electrons) and annihilates a large SIE that describes actually useful non-dynamic electron correlation thus leading to a deterioration rather than an improvement of the DFT description. This is also true in the case of any transition state for a bond breaking or forming process.

(b) Even in the case of the breaking of an odd-electron bond, a SIE-free DFT method will no longer account for the long-range bond correlation effects needed for the balanced description of ionic and covalent dissociation limits. Hence SIC-DFT cannot describe the dissociation of radical cations correctly.

(c) In this work, we have shown that the SIE for bonds formed by electron-rich atoms accounts for a large amount of dynamic electron correlation, which is true for odd- as well as even-electron bonds. In the latter case these extra-effects help to improve the description of the breaking of electron-pair bonds. SIC-DFT can no longer provide these improvements.

(d) SIC-DFT improves the description of intraelectronic exchange, but still suffers from the simplified description of interelectronic exchange, which can lead to an unbalanced description of different states. HF interelectronic exchange comprises long-range effects, which are missing in SIC-DFT.

A balanced DFT functional must fulfill two, apparently contradictory, requirements: (i) In odd-electron situations, the SIE for the delocalized electron has to be eliminated. (ii) In situations where the KS reference function misses non-dynamic correlation effects (typically in the recoupling region of breaking or forming electron-pair bonds), the SIE must be retained. Conventional hybrid functionals are a compromise between (i) and (ii). Hence, a reparametrization of hybrid functionals can just improve the description of a certain type of system at the cost of others. SIC-DFT obeys (i) but ignores (ii) completely. An early attempt to obey both (i) and (ii) has been made by Burke and co-workers,[72] where a_{HF} is not fixed in advance but determined case by case depending on the character of the system investigated.

Recently, a number of SIE-free DFT functionals outside the framework of the PZ formalism have been suggested.[41,42] These functionals are unitary invariant and computationally much less demanding than the PZ formalism. They use iso-electron indicators, *i.e.* local functions of the density, the KS density matrix, and their gradients, to probe the molecule for regions with one-electron behavior and eliminate the SIE in these regions. The question arises whether these functionals obey (i) and (ii). In the same way as PZ-SIC, these methods are focused on obeying (i), however no particular measures are taken to fulfill (ii). The local hybrid (lh) functional by Jaramillo and co-workers,[42] for instance, is constructed such that it turns into pure DFT for metallic situations, *i.e.* situations with small relative density gradients. The values for r_e and D_e of **1–6** obtained with the lh functional from ref. 42 are superior to the values obtained with standard BLYP or B3LYP but generally inferior to the SC-SIC-BLYP results. Furthermore, it is stated in ref. 42 that the lh functionals are clearly inferior to standard BLYP and B3LYP for the calculation of atomization energies. It turns out that the lh functionals overestimate the portion of exact exchange required for a balanced suppression of the SIE. It appears possible in principle to obey (ii) with a functional using local correlation indicators, however, so far there is no such functional and no appropriate indicator that could detect bond-breaking and similar situations.

From the results obtained in this work, we conclude that the best way of eliminating all SIE-related problems is to use exact exchange throughout in DFT calculations. This implies that all short- and long-range correlation effects discussed in connection with DFT exchange have to be added to the correlation functional. It is known that such a HF-KS approach performs poorly for LDA and GGA correlation functionals, and it has been pointed out[73] that it is clearly inferior to pure GGA even if the most advanced semi-local correlation functionals are used. Only in connection with a truly nonlocal correlation functional can exact exchange provide results superior to methods employing local or semilocal exchange. Two ways seem to be prospective to construct such a truly nonlocal correlation functional. First, one could include the DFT exchange functional into the correlation functional using eqn. (4):

$$\mathrm{XC} = \mathrm{X(exact)} + [c_1\mathrm{C(DFT)} + c_2\mathrm{X(DFT)} - c_3\mathrm{X(exact)}] \quad (4)$$

The XC functional (4) must fulfill the sum rule, *i.e.* the new correlation functional must integrate to zero, which means $c_1 = c_2$. For constant c_1, c_2, eqn. (4) is just a reformulation of hybrid-GGA. If, however, c_1, c_2 are variable in space, eqn. (4) is a sound starting point for the description of long-range correlation effects with the help of the long-ranged exact exchange. According to Perdew and Schmidt,[73] functional (4) would belong to the hyper-GGA functionals of the "Jacob's ladder".

Another possibility would be to derive correlation functionals from high level *ab initio* calculations in the spirit of Colle and Salvetti[74] with the requirement that they account for all needed short- and long-range Coulomb correlation. There is work in progress in this direction, however it is too early to see a realization that solves all the problems in connection with the standard XC functionals discussed in this work.

Clearly, there is always the possibility to make the XC functional orbital dependent and to introduce specific correlation effects needed *via* the virtual orbitals and to obtain in this way (at least partially) correct correlation, *i.e.*, to construct a functional that is on the fifth rung of the "Jacob's ladder".[73] However, this will be only reasonable if the numerical expenses of such a functional are significantly smaller than those of correlated wave-function methods.

Appendix

The error in the DFT description of the interelectronic exchange results in an artificial stabilization of the covalent state relative to the ionic one. For the purpose of proving this a symmetric radical cation at an interaction distance R large enough to keep the fragments well separated from each other is considered. The electron densities at the two fragments (excluding the bonding β electron) are denoted by ϱ_A^c and ϱ_B^c. If the bonding valence electron is at fragment A or B, its density in the covalent state will be ϱ_A^v or ϱ_B^v, respectively. The valence density at the two fragments is $(\varrho_A^v + \varrho_B^v)/2$. (We neglect orbital relaxations between covalent and ionic state).

The exact interelectronic exchange between two orbitals is bilinear in the densities of the orbitals. Consequently, the interelectronic exchange between the bonding electron and the remaining electrons is the same no matter whether the valence density is located at fragment A, fragment B, or one half of it at each fragment. The interelectronic exchange within the fragments is not affected by the transition from the ionic to the covalent state. Altogether, exact wavefunction theory gives the same interelectronic exchange for ionic and covalent state.

For the LDA exchange, the interatomic exchange energies of covalent and ionic state become

$$E_{X,inter,ion}^{DFT} = -C_X \int d^3r\{[(\varrho_A^v(\boldsymbol{r}) + \varrho_A^c(\boldsymbol{r})]^{4/3} - \varrho_A^v(\boldsymbol{r})^{4/3} + \varrho_B^c(\boldsymbol{r})^{4/3}\} - \Delta, \quad \text{(A1a)}$$

$$E_{X,inter,cov}^{DFT} = -C_X \int d^3r\left\{\left[\frac{1}{2}\varrho_A^v(\boldsymbol{r}) + \varrho_A^c(\boldsymbol{r})\right]^{4/3} - \frac{1}{2}\varrho_A^v(\boldsymbol{r})^{4/3} + \left[\frac{1}{2}\varrho_B^v(\boldsymbol{r}) + \varrho_B^c(\boldsymbol{r})\right]^{4/3} - \frac{1}{2}\varrho_B^v(\boldsymbol{r})^{4/3}\right\} - \Delta. \quad \text{(A1b)}$$

Factor $C_X = (3/2)(3/4\pi)^{1/3}$. Δ is the intraelectronic exchange for all core electrons in fragments A and B, which is the same for ionic and covalent state. Because of the symmetry of fragments A and B, ϱ_B^c, ϱ_B^v can be replaced by ϱ_A^c, ϱ_A^v, and the difference between $E_{X,inter,ion}^{DFT}$ and $E_{X,inter,cov}^{DFT}$ is

$$E_{X,inter,ion}^{DFT} - E_{X,inter,cov}^{DFT} = -C_X \int d^3r\left[\xi(\varrho_A^v(\boldsymbol{r}); \varrho_A^c(\boldsymbol{r})) + \xi(0; \varrho_A^c(\boldsymbol{r})) - 2\xi\left(\frac{1}{2}\varrho_A^v(\boldsymbol{r}); \varrho_A^c(\boldsymbol{r})\right)\right], \quad \text{(A2a)}$$

where the function ξ is defined as

$$\xi(x; y) = (x + y)^{4/3} - y^{4/3}. \quad \text{(A2b)}$$

For any fixed positive value of y and all positive values x, $\partial^2\xi/\partial x^2 < 0$ for all x, *i.e.*, ξ is a concave function of x. This implies

$$\xi(x; y) + \xi(0; y) - 2\xi(x/2; y) < 0 \text{ for all } x, y > 0. \quad \text{(A3)}$$

Hence, the integrand in eqn. (A2a) is always negative, and consequently $E_{X,inter}^{DFT}$ is more positive for the ionic than for the covalent state. As a correct description should give the same interelectronic exchange energy for ionic and covalent state, this result shows that LDA overstabilizes the covalent state relative to the ionic one. The result can be generalized to GGA, keeping in mind that the LDA term is the dominating contribution to the GGA exchange energy.

It should be noted that the overstabilization of the covalent state due to the interelectronic exchange is independent of R as long as R is large enough to keep the fragments separated. There is no $1/R$ dependence as in the case of the SIE.

Acknowledgements

We thank Victor Polo for carrying out preliminary calculations for this project. This work was supported by the Swedish Research Council (Vetenskapsrådet). An allotment of computer time at the National Supercomputer Center (NSC) at Linköping is gratefully acknowledged. J.G. thanks Carl Tryggers Stiftelse for financial support.

References

1 P. Hohenberg and W. Kohn, *Phys. Rev.*, 1964, **136**, B864–B871.
2 W. Kohn and L. J. Sham, *Phys. Rev.*, 1965, **140**, A1133–A1138.
3 J. P. Perdew and A. Zunger, *Phys. Rev. B*, 1981, **23**, 5048–5079.
4 (*a*) J. P. Perdew, *Local Density Approximations in Quantum Chemistry and Solid State Physics*, ed. J. Avery and J. P. Dahl, Plenum Press, New York, 1984; (*b*) J. P. Perdew, M. Ernzerhof, *Electronic Density Functional Theory: Recent Progress and New Directions*, ed. J. F. Dobson, G. Vignale and M. P. Das, Plenum Press, New York, 1998, p. 31.
5 D. Cremer, *Mol. Phys.*, 2001, **99**, 1899–1940.
6 V. Polo, E. Kraka and D. Cremer, *Mol. Phys.*, 2002, **100**, 1771–1790.
7 V. Polo, E. Kraka and D. Cremer, *Theor. Chem. Acc.*, 2002, **107**, 291–303.
8 V. Polo, J. Gräfenstein, E. Kraka and D. Cremer, *Chem. Phys. Lett.*, 2002, **352**, 469–478.
9 V. Polo, J. Gräfenstein, E. Kraka and D. Cremer, *Theor. Chem. Acc.*, 2003, **109**, 22–35.
10 D. Cremer, M. Filatov, V. Polo, E. Kraka and S. Shaik, *Int. J. Mol. Sci.*, 2002, **3**, 604–638.
11 J. Gräfenstein, E. Kraka and D. Cremer, *J. Chem. Phys.*, 2004, **120**, 524–539.
12 L. Noodleman, D. Post and E. J. Baerends, *Chem. Phys.*, 1982, **64**, 159–166.
13 (*a*) J. G. Harrison, R. A. Heaton and C. C. Lin, *J. Phys. B*, 1983, **16**, 2079–2091; (*b*) M. R. Pederson, R. A. Heaton and C. C. Lin, *J. Chem. Phys.*, 1984, **80**, 1972–1975; (*c*) M. R. Pederson, R. A. Heaton and C. C. Lin, *J. Chem. Phys*, 1985, **82**, 2688–2699.
14 (*a*) J. B. Krieger and Y. Li, *Phys. Rev. A*, 1989, **39**, 6052–6055; (*b*) Y. Li and J. B. Krieger, *Phys. Rev. A*, 1990, **41**, 1701–1704; (*c*) J. Chen, J. B. Krieger and Y. Li, *Phys. Rev. A*, 1996, **54**, 3939–3947.
15 (*a*) Y. Guo and M. A. Whitehead, *J. Comput. Chem.*, 1991, **12**, 803–810; (*b*) M. A. Whitehead, S. Suba, *Recent Advances in Computational Chemistry - Vol. 1, Recent Advances in Density Functional Methods, Part I*, ed. D. P. Chong, World Scientific, Singapore, 1995, p. 53.
16 B. G. Johnson, C. A. Gonzales, P. M. W. Gill and J. A. Pople, *Chem. Phys. Lett.*, 1994, **221**, 100–108.
17 S. Goedecker and C. J. Umrigar, *Phys. Rev. A*, 1997, **55**, 1765–1771.
18 M. A. Buijse and E. J. Baerends, *Theor. Chim. Acta*, 1991, **79**, 389–401; *J. Chem. Phys.*, 1990, **93**, 4129–4141.
19 (*a*) X. M. Tong and S. I. Chu, *Phys. Rev. A*, 1997, **55**, 3406–3416; (*b*) X. M. Tong and S. I. Chu, *Phys. Rev. A*, 1998, **57**, 855–863; (*c*) T. F. Jiang, X. M. Tong and S. I. Chu, *Phys. Rev. B*, 2001, **63**, 45 317
20 (*a*) R. K. Nesbet, *Phys. Rev. A*, 1997, **56**, 2665–2669; (*b*) R. K. Nesbet, *Int. J. Quantum Chem.*, 2001, **85**, 405–410.
21 (*a*) G. I. Csonka, N. A. Nguyen and I. Kolossvary, *J. Comput. Chem.*, 1997, **18**, 1534–1545; (*b*) G. I. Csonka and B. G. Johnson, *Theor. Chem. Acc.*, 1998, **99**, 158–165.
22 K. Burke, J. P. Perdew and M. Ernzerhof, *J. Chem. Phys.*, 1998, **109**, 3760–3771.
23 (*a*) O. V. Gritsenko, B. Ensing, P. R. T. Schipper and E. J. Baerends, *J. Phys. Chem. A*, 2000, **104**, 8558–8565; (*b*) See also O. V. Gritsenko, P. R.T. Schipper and E. J. Baerends, *J. Chem. Phys.*, 1997, **107**, 5007–5015; (*c*) P. R.T. Schipper, O. V. Gritsenko and E. J. Baerends, *Phys. Rev. A*, 1998, **57**, 1729–1742.
24 (*a*) J. Garza, J. A. Nichols and D. A. Dixon, *J. Chem. Phys.*, 2000, **112**, 7880–7890; (*b*) J. Garza, J. A. Nichols and D. A. Dixon, *J. Chem. Phys.*, 2000, **113**, 6029–6034; (*c*) J. Garza, R. Vargas, J. A. Nichols and D. A. Dixon, *J. Chem. Phys.*, 2001, **114**, 639–651.
25 F. della Sala and A. Görling, *J. Chem. Phys.*, 2001, **115**, 5718–5732.
26 (*a*) S. Patchkovskii, J. Autschbach and T. Ziegler, *J. Chem. Phys.*, 2001, **115**, 26–42; (*b*) S. Patchkovskii and T. Ziegler, *J. Phys. Chem. A*, 2002, **106**, 1088–1099.

27 S. Kümmel and J. P. Perdew, *Mol. Phys.*, 2003, **101**, 1363–1368.
28 E. Fermi and E. Amaldi, *Accad. Ital. Rome*, 1934, **6**, 117–149.
29 J. C. Slater, *Quantum Theory of Molecules and Solids (The Self-consistent Field for Molecules and Solids) Vol. 4*, McGraw Hill, New York, 1974.
30 (*a*) For a summary, see A. D. Becke, in *Advanced Series in Physical Chemistry*, ed. D. R. Yarkony, Modern Electronic Structure Theory, Part II, World Scientific, Singapore, 1995, vol. 2, p. 1022; (*b*) A. D. Becke, *J. Chem. Phys.*, 1996, **104**, 1040–1046.
31 R. Merkle, A. Savin and H. Preuss, *J. Chem. Phys.*, 1992, **97**, 9216–9221.
32 E. Ruiz, D. R. Salahub and A. Vela, *J. Phys. Chem.*, 1996, **100**, 12 265–12 276.
33 T. Bally and G. N. Sastry, *J. Phys. Chem. A*, 1997, **101**, 7923–7925.
34 (*a*) B. Braïda and P. C. Hiberty, *J. Phys. Chem. A*, **102**, 7872–7877; (*b*) B. Braïda, D. Lauvergnat and P. C. Hiberty, *J. Chem. Phys.*, 2001, **115**, 90–102.
35 (*a*) Y. Zhang and W. Yang, *J. Chem. Phys.*, 1998, **109**, 2604–2608; (*b*) Y. Zhang and W. Yang, *Theor. Chem. Acc.*, 2000, **103**, 346–348.
36 M. Sodupe, J. Bertran, L. Rodríguez-Santiago and E. J. Baerends, *J. Phys. Chem.*, 1999, **103**, 166–170.
37 Y. Xie, H. F. Schaefer III, X. Y. Fu and R. Z. Liu, *J. Chem. Phys.*, 1999, **111**, 2532–2541.
38 H. Chermette, I. Ciofini, F. Mariotti and C. Daul, *J. Chem. Phys.*, 2001, **114**, 1447–1453.
39 M. Grüning, O. V. Gritsenko, S. J. A. van Gisbergen and E. J. Baerends, *J. Phys. Chem.*, 2001, **105**, 9211–9218.
40 S. Patchkovskii and T. Ziegler, *J. Chem. Phys.*, 2002, **116**, 7806–7813.
41 A. Becke, *J. Chem. Phys.*, 2000, **112**, 4020–4026.
42 J. Jaramillo, G. E. Scuseria and M. Ernzerhof, *J. Chem. Phys.*, 2003, **118**, 1068–1073.
43 J. M. Foster and S. F. Boys, *Rev. Mod. Phys.*, 1960, **32**, 300–302.
44 E. Kraka, J. Gräfenstein, M. Filatov, J. Gauss, A. Wu, V. Polo, Y. He, F. Reichel, L. Olsson, Z. Konkoli, Z. He and D. Cremer, Cologne 2003, Göteborg University, Göteborg, 2003.
45 A. D. Becke, *Phys. Rev. A*, 1988, **38**, 3098–3100.
46 C. Lee, W. Yang and R. G. Parr, *Phys. Rev. B*, 1988, **37**, 785–789.
47 A. D. Becke, *J. Chem. Phys.*, 1993, **98**, 5648–5652.
48 A. D. Becke, *J. Chem. Phys.*, 1993, **98**, 1372–1377.
49 K. Raghavachari, G. W. Trucks, J. A. Pople and M. Head-Gordon, *Chem. Phys. Lett.*, 1989, **157**, 479–483.
50 T. H. Dunning, Jr., *J. Chem. Phys.*, 1989, **90**, 1007–1023.
51 J. C. Slater, *Phys. Rev.*, 1951, **81**, 385–390.
52 S. H. Vosko, L. Wilk and M. Nusair, *Can. J. Phys.*, 1980, **58**, 1200–1211.
53 J. P. Perdew, in P. Ziesche and H. Eschrig, *Electronic Structure of Solids '91*, Akademie-Verlag, Berlin, 1991, p. 11; J. P. Perdew, Y. Wang, *Phys. Rev. B*, 1992, **45**, 13 244–13 249.
54 J. P. Perdew, *Phys. Rev. B*, 1986, **33**, 8822–8824.
55 C. Adamo and V. Barone, *J. Chem. Phys.*, 1998, **108**, 664–675.
56 J. A. Pople, J. S. Binkley and R. Seeger, *Int. J. Quantum Chem. Symp.*, 1976, **10**, 1–19.
57 (*a*) Z. Konkoli and D. Cremer, *Int. J. Quantum Chem.*, 1998, **67**, 1–9; (*b*) Z. Konkoli and D. Cremer, *Int. J. Quantum Chem.*, 1998, **67**, 29–40; (*c*) D. Cremer, J. A. Larsson, and E. Kraka, in *Theoretical and Computational Chemistry*, Theoretical Organic Chemistry, ed. C. Párkányi, Elsevier, Amsterdam, 1998, vol. 5, p. 259.
58 R. Seeger and J. A. Pople, *J. Chem. Phys.*, 1977, **66**, 3045–3050.
59 R. Bauernschmitt and R. Ahlrichs, *Chem. Phys.*, 1996, **104**, 9047–9052.
60 J. F. Stanton, J. Gauss, J. D. Watts, W. J. Lauderdale and R. J. Bartlett, ACES II, Quantum Theory Project, University of Florida, 1992; See also J. F. Stanton, J. D. Watts, W. J. Lauderdale, R. J. Bartlett, *Int. J. Quantum Chem. Symp.*, 1992, **26**, 879–894.
61 M. J. Frisch, G. W. Trucks, H. B. Schlegel, G. E. Scuseria, M. A. Robb, J. R. Cheeseman, V. G. Zakrzewski, J. A. Montgomery, Jr., R. E. Stratmann, J. C. Burant, S. Dapprich, J. M. Millam, A. D. Daniels, K. N. Kudin, M. C. Strain, O. Farkas, J. Tomasi, V. Barone, M. Cossi, R. Cammi, B. Mennucci, C. Pomelli, C. Adamo, S. Clifford, J. Ochterski, G. A. Petersson, P. Y. Ayala, Q. Cui, K. Morokuma, D. K. Malick, A. D. Rabuck, K. Raghavachari, J. B. Foresman, J. Cioslowski, J. V. Ortiz, B. B. Stefanov, G. Liu, A. Liashenko, P. Piskorz, I. Komaromi, R. Gomperts, R. L. Martin, D. J. Fox, T. Keith, M. A. Al-Laham, C. Y. Peng, A. Nanayakkara, C. Gonzalez, M. Challacombe, P. M. W. Gill, B. Johnson, W. Chen, M. W. Wong, J. L. Andres, C. Gonzalez, M. Head-Gordon, E. S. Replogle and J. A. Pople, Gaussian 98, Revision A.9, Gaussian Inc., Pittsburgh PA, 1998.
62 C. Møller and M. S. Plesset, *Phys. Rev.*, 1934, **46**, 618–622; For a recent review, see D. Cremer, in *Encyclopaedia of Computational Chemistry*, ed. P.v.R. Schleyer, N.L. Allinger, T. Clark, J. Gasteiger, P.A. Kollman, H. F Schaefer III, and P.R. Schreiner, John Wiley, Chichester, UK, 1998 vol. 3, p. 1706.
63 (*a*) For reference values, see (a) B. S. Jursic, *J. Mol. Struct. (THEOCHEM)*, 1998, **427**, 117–121; (*b*) For the poor performance of DFT, see (b) B. Jursic, *J. Mol. Struct. (THEOCHEM)*, 1998, **430**, 17–22.
64 P. R. T. Schipper, O. V. Gritsenko and E. J. Baerends, *J. Chem. Phys.*, 1999, **111**, 4056–4067.
65 A. Wu, D. Cremer and B. Plesnicar, *J. Am. Chem. Soc.*, 2003, **125**, 9395–9402.
66 B. Plesnicar, T. Tuttle, J. Cerkovnik, J. Koller and D. Cremer, *J. Am. Chem. Soc.*, 2003, **125**, 11 553–11 564.
67 (*a*) D. Porezag and M. R. Pederson, *J. Chem. Phys.*, 1995, **102**, 9346–9349; (*b*) J. Baker, M. Muir, J. Andzelm and A. Scheiner, in *ACS Symposium Series*, "Chemical Applications of Density Functional Theory", ed. B.B. Laird, R.B. Ross and T. Ziegler, 1995, vol. 629, p. 342, and references cited therein.
68 (*a*) M. Wirstam, M. R. A. Blomberg and P. E. M. Siegbahn, *J. Am. Chem. Soc.*, 1999, **121**, 10178–10185; (*b*) P. E. M. Siegbahn, *J. Comput. Chem.*, 2001, **22**, 1634–1645; (*c*) A. Bassan, M. R. A. Blomberg, P. E. M. Siegbahn and L. Que, Jr., *J. Am. Chem. Soc.*, 2002, **124**, 11 056–11 063.
69 R. Wrobel, W. Sander, E. Kraka and D. Cremer, *J. Phys. Chem. A*, 1999, **103**, 3693–3705.
70 J. Gräfenstein, E. Kraka, M. Filatov and D. Cremer, *Int. J. Mol. Sci.*, 2002, **3**, 360–394.
71 V. Sychrovský, J. Gräfenstein and D. Cremer, *J. Chem. Phys.*, 2000, **113**, 3530–3547.
72 K. Burke, M. Ernzerhof and J. P. Perdew, *Chem. Phys. Lett.*, 1997, **265**, 115–120.
73 J. P. Perdew and K. Schmidt, *Density Functional Theory and its Application to Materials*, ed. V.E. Van Doren, K. Van Alsenoy and P. Geelings, American Institute of Physics, 2001.
74 (*a*) R. Colle and O. Salvetti, *Theor. Chim. Acta*, 1975, **37**, 329–334; (*b*) R. Colle and O. Salvetti, *Theor. Chim. Acta*, 1979, **53**, 55–63.

